A new technique for the investigation of high energy cosmic rays

S. Kisdnasamy

A NEW TECHNIQUE FOR THE INVESTIGATION OF HIGH ENERGY COSMIC RAYS

A thesis Presented by

S. Kisdnasamy

For the Degree of Doctor of Philosophy

at

The University of Durham.

December, 1958.

A NEW TECHNIQUE FOR THE INVESTIGATION OF HIGH ENERGY COSMIC RAYS.

Ph.D Thesis submitted by S. Kisdnasamy

December, 1958.

ABSTRACT

A technique has been developed for the precise location of cosmic rays in a magnetic spectrograph. The technique uses the neon flash tube first introduced by Conversi and his co-workers. In this technique ionising particles give rise to visible flashes in a glass tube containing neon.

The thesis describes a systematic study of the flash tubes over a wide range of parameter. Tubes have been constructed having the properties required for operation in a spectrograph and a description is given of the operation of a prototype spectrograph. The accuracy of track location has been found to be at least as great as that in conventional cloud chambers.

The theoretical aspect of the operation of the tubes is discussed and a new mechanism is postulated for tubes filled at high pressures.

The design and construction of part of the large spectrograph is described.

CONTENTS

PREFACE

This thesis describes the development of a new technique for the detection of ionising particles and its use in an instrument for the investigation of high energy cosmic rays.

The development and some preliminary measurements on the characteristics of the neon flash tubes were made by the author at Manchester. The work was continued in Durham by the author and his colleagues under the supervision of Dr. A. W. Wolfendale.

In what follows emphasis is placed on those aspects of the work which were the particular concern of the author. Acknowledgement is made in the text to any specific contribution made by his colleagues.

Some of the work described has been published by the author and his colleagues. (Gardener et al 1957, Ashton et al 1958).

CHAPTER I

INTRODUCTION

The existence of cosmic radiation has been known since the early experiments of Hess (1912, 15) and Kolhorster (1914-19). From more recent measurements made at high altitudes with nuclear emulsions and counter telescopes it has been established that the primary cosmic rays entering the earth's atmosphere consist mainly of protons and nuclei of the heavier elements. The primary nuclei are absorbed by inelastic collisions with air nuclei. The absorption length for nucleons is ~ 120 g/cm^2 and is considerably shorter for α particles and heavier nuclei; in consequence most of the primary cosmic rays interact in the upper layers of the atmosphere (above $\sim 50,000$ ft.). These interactions give rise to the secondary radiation consisting of nucleons and nuclear fragments, charged and neutral π - mesons, and heavy mesons and hyperons. The secondary particles produce further mesons and nucleons by collisions with air nuclei. The positive and negative π - mesons have a mean-life of $(2.56 \pm .05) \times 10^{-8}$ sec and either decay in flight into μ - mesons and neutrinos or are absorbed by nuclei in inelastic collicions somewhat similar to those of the primary nucleons. The relative probabilities of these processes can be evaluated as follows.

If τ is the mean life of the meson at rest its apparent mean life when moving with a velocity βc is $\tau/(1-\beta^2)^{\frac{1}{2}}$. The average distance traversed by the meson before it disintegrates is thus

$$Z_d = \frac{\beta c \tau}{\left[1-\beta^2\right]^{1/2}} = \frac{p\tau}{m}$$

where p is the momentum of the meson and m is the rest mass. For a π- meson of rest mass 139. 65 $\pm$ .06 M.e.v. having an energy of p_G G.e.v. the distance Zd is $\sim 50\, p_G$ metres.

The probability of interaction of the π-meson can be derived under certain simplifying assumptions. It can be assumed that the π-mesons are produced at a unique pressure level of 100 g/cm2 below the top of the atmosphere corresponding to 15 kilometres above sea level. The interaction length, as distinct from the absorption length, has been found to be ~ 60 g/cm^2 at low energies and it is assumed that this result is applicable to all energies. The mean free path before interaction is then ~ 3000 metres. Thus, since Zd $\sim 50\, p_G$ metres, decay and interaction are equally probable for $p_G \sim 20$ G.e.v/c. This means that most of the π-mesons with momentum appreciably below 20 G.e.v/c and a small fraction of those above 20 G.e.v/c decay into μ-mesons.

Although the nuclear interaction of the μ-meson is weak and most of the fast μ mesons produced by π-decay reach sea level and the fact that the μ- meson is unstable and decays into an electron and two neutrinos results in a loss of low energy μ- mesons.

The neutral π- mesons have a short mean life of $\sim 10^{-16}$ sec and decay into two photons which in turn materialise in the presence of nuclei to form electron pairs and ultimately electron photon cascades.

The heavy mesons and hyperons are produced in relatively small numbers and are unstable, having numerous decay schemes.

Of particular relevance to the present discussion is the nature of the cosmic radiation at, or near, sea level. It is customary to divide this radiation into two components, the hard and soft components, so named because of their ability or otherwise to penetrate moderate thicknesses (10 cm) of lead. The hard component consists predominantly of μ^- mesons. At low energies μ^- mesons come chiefly from the $\pi^- - \mu$ decay process. High energy μ^- mesons arise from the decay of π^- mesons and also from the $k\mu_2$, $k\mu_3$ and perhaps other heavy mesons. The soft component consists mainly of electrons and photons and comes from the decay of π^0 mesons, the decay of μ^- mesons and ejection of electrons from oxygen and nitrogen molecules by the energetic μ^- mesons.

The hard component at sea level has been studied in detail by many workers. In particular the momentum spectrum and the ratio of positive to negative μ^- mesons have been extensively investigated. Such investigations are useful in that they throw light on the basic interactions of the primaries and when combined with underground measurements give information on the energy loss of fast μ^- mesons.

The work described in this thesis concerns the design and construction of an instrument for studying the sea level μ^- mesons, especially the determination of their momentum spectrum.

CHAPTER II

COSMIC-RAY SPECTROGRAPHS

II.1 Previous Instruments

Measurements of the energy spectrum have been made using two main methods, viz: the determination of range and momentum.

Absolute measurements have been made of the flux of μ-mesons as a function of minimum range for various condensed materials. Among the early experiments of this type may be mentioned those of Wilson (1938) and Ehmert (1937) who used counter telescopes under different thicknesses of absorber. The range-energy relationship was then used to convert the range spectrum to the momentum spectrum at sea level. This method suffers from the disadvantages that the range energy relation is uncertain at high energies and a rather low limiting momentum is set by the maximum thickness of absorber available.

Blackett (1937), Jones (1939) and Wilson (1946) used cloud chambers operated in magnetic fields to determine the momenta of fast particles. The differential spectrum of fast μ-mesons at sea level was thus directly determined. This method, too, has defects in that cloud chambers in magnetic fields are inefficient in making full use of the magnetic field available. Furthermore, turbulence in the cloud chamber sets a comparatively low upper limit to the measurable momenta

In recent years the differential spectrum has been measured with magnetic spectrographs in which most of the detecting elements are external

to the magnetic field. Alikanian and co-workers (1947, a,b, 1948 a,b) & Caro et al (1950) used counter spectrographs with one magnet and the Manchester group, Hyams et al (1950), a symmetrical arrangement of two magnets. The efficiency with which the available magnetic field was used in the latter instrument was 50% compared with 5% in cloud chamber work (Hyams et al 1950). The principle of spectrograph operation can best be discussed with reference to one particular instrument and the Manchester spectrograph will be taken as an example.

II.2. The Manchester Spectrograph.

This instrument consisted of two large electromagnets each with pole faces of area 50 cm x 40 cm, with the smaller dimension vertical and the pole faces separated by a distance of 9.5 cm. Three trays of Geiger counters determined the points of intersection of the particle trajectory with the three planes aa', bb', cc'. A schematic diagram of the arrangement is shown in fig. 1. The shaded portions represent the magnetic field regions. To exclude particles which in any part of their trajectory may pass through the iron of the pole pieces, defining counters were placed in each pole gap. The accepted event of the spectrograph was thus a five-fold coincidence comprising discharges of one counter from each of the three trays a, b and c and one defining counter from each of the trays in the pole gaps of the magnets.

The principle of operation can be seen by reference to fig. 1. The angular deflection θ of the particle in each of magnetic fields is given by

$$\theta = \frac{\int H\,d\ell}{\rho} = \frac{300 \int H\,d\ell}{p}$$

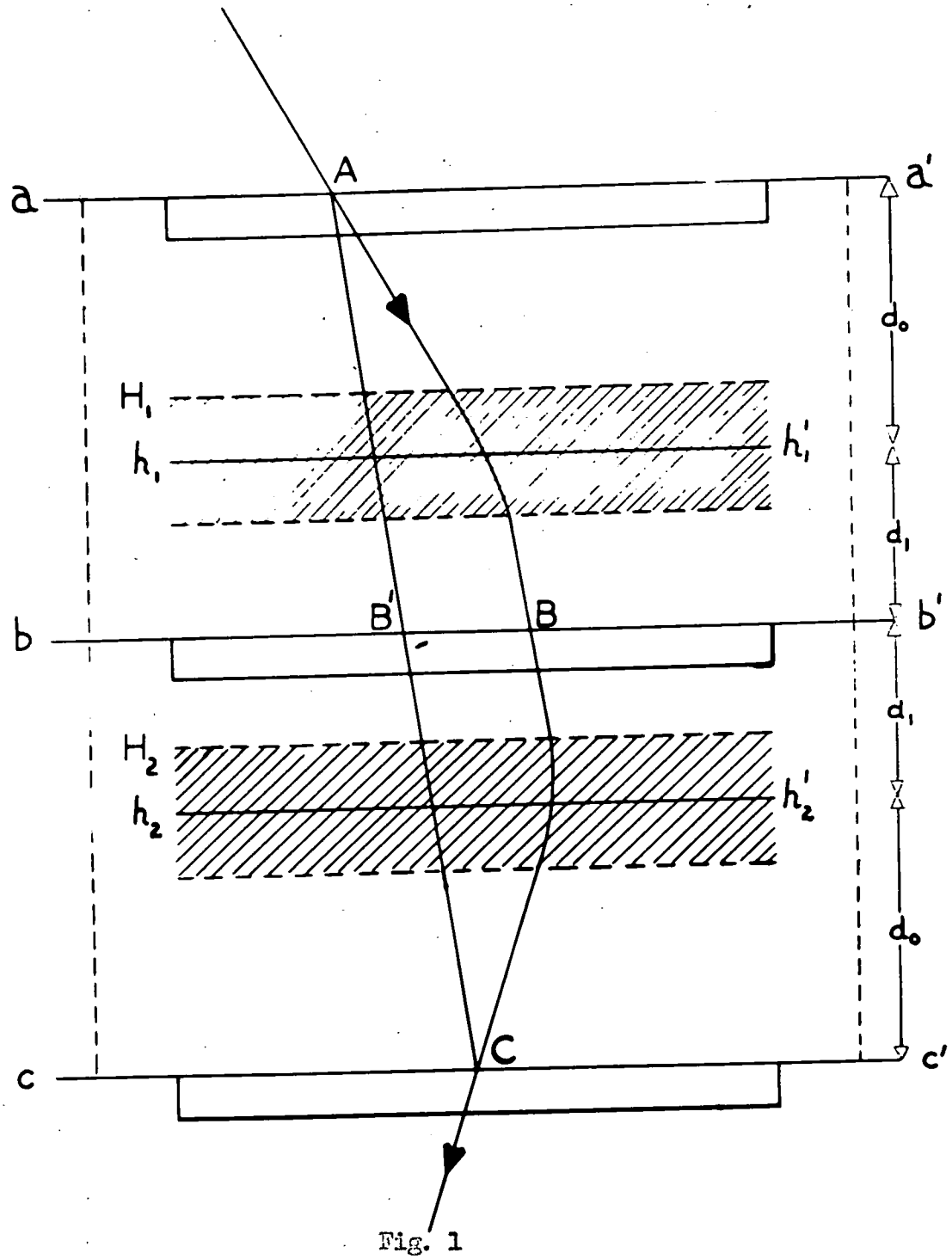

Fig. 1

Schematic diagram of the Manchester Spectrograph

where ρ is the radius of curvature of the particle trajectory in cm, p the momentum of the particle in e.v./$_c$ and $\int H dl$ is the line integral of the magnetic field in gauss cm. It can be shown that the sagittal deflection BB' = Δ = do Θ. Thus the momentum of the particle in terms of Δ is

$$p = \frac{300\, d_o \int H dl}{\Delta}$$

With the maximum value for $\int H dl$ of 6 x 10^3 gauss cm and counters of 4 cm diameter the maximum detectable momentum is 50 G.e.v./$_c$. The maximum detectable momentum is defined as the momentum for which the magnetic deflection is equal to the r.m.s. uncertainty in the measurement of the deflection.

In order to increase the maximum detectable momentum Holmes et al (1956) introduced a flat cloud chamber at each of the three measuring level a, b, c. The tracks in these cloud chambers had a width of ~1 mm and it was possible with careful temperature control to locate the trajectory of the particle with an overall uncertainty of ~0.8 mm (Lloyd and Wolfendale 1957). With this new arrangement the maximum detectable momentum was ~500 G.e.v/c.

The use of two magnets and the geometry employed in the Manchester spectrograph restricted the rate of particles to ~16 hr^{-1}. The limit to the number of events in the latter arrangement was set rather by the time taken in the analysis than the time for collection.

To increase the rate of collection of particles of high momenta the most obvious solution is to increase the available solid angle by dispensing

with one magnet. However, in order to achieve comparable momentum resolution, higher accuracy of track determination is required. In the next chapter there is considered in detail the design of an instrument of high flux and high maximum detectable momentum.

CHAPTER III

THE DESIGN OF A HIGH FLUX SPECTROGRAPH OF HIGH RESOLUTION.

III. 1. General Design Considerations

The problem is to design a spectrograph, with a magnet of the Manchester type, having a rate higher by a factor of ~10 and a maximum detectable momentum of at least 1000 G.e.v/c. The basic requirements of the instruments are thus (a) a large solid angle of particle collection, (b) the largest possible line integral of the magnetic field and (c) a high accuracy of track location in the detectors. The large solid angle of acceptance and thus high flux is automatically achieved by using only one of the deflecting magnets and large areas of detection. Some increase in the value of the line integrals $\int H d\ell$ is obtained by operating the magnet at a higher current rating, viz. 70 amperes per coil at 30 k.w. to give a central field of 13,000 gauss. The problem, therefore, reduces to finding a suitable particle detector which could give the high accuracy of track location.

As particle detectors, any of the following can be used: Geiger counters, cloud chambers, spark counters or scintillation counters. The requirements of the detector are that it should have a large area, a high spatial resolution, good time resolution and be of low cost and simple in construction and operation.

Geiger counters of large area and adequate time resolution are easily constructed, but track location to 0.5 mm can only be obtained by many overlapping layers of small diameter (5 mm) counters. Since a very large

number of such counters is needed to cover an area 1000 cm^2, the cost of the equipment will be prohibitive.

Cloud chambers have high spatial and time resolution, but large flat chambers present considerable difficulties both in construction and operation. A fundamental objection is the inherent instability of the cloud chamber track leading to a variability in the maximum detectable momentum.

The early spark counters of Pidd and Madansky (1949), Robinson (1953) have been improved by Cranshaw and de Beer (1957). Cranshaw and de Beer have successfully operated a spark counter of area 100 cm^2 to locate the trajectories of fast cosmic ray particles. However, it is not known whether it is possible to operate efficiently counters of large area (10,000 cm^2) over long periods of time. Furthermore, spark counters are not efficient in locating the trajectories of associated events. Again when several particles are incident on the spark counter the spark occurs preferentially along the track of the particle having a higher specific ionisation and consequently all the particles are not detected.

Scintillation counters of large area and good time resolution are easily constructed. But to obtain a high spatial resolution, a large number of small diameter (5 mm) scintillators is required. The cost of the electronic equipment such as photomultipliers, stabilized power supplies etc., will be prohibitive.

On the other hand, the neon flash tube of Conversi et al (1955) in which the spark is replaced by a localised glow discharge, appears to have

many advantages. In this technique neon is contained in sealed glass tubes placed between parallel, conducting electrodes. If a high voltage pulse is applied soon after the passage of an ionising particle a visible glow discharge results. Long tubes of small diameter can be used and the flash photographed. It is obvious that this technique is essentially simple and most of the spectrograph requirements are satisfied.

III. 2. Experiments of Conversi et al on the Neon Flash Tube.

Conversi's flash tube consisted of a thin glass tube, internal diameter 6.5 mm, external diameter 7.0 mm, length 21.5 cm, containing spectroscopic neon at a pressure of 35 cm Hg. Four layers of tubes were placed between aluminium electrodes. Two Geiger counters placed above and below the assembly were used to select ionising particles traversing the sensitive volume of the assembly. The two-fold coincidence of these counters triggered a pulse generator after a few microseconds delay (T_D), which then applied a 20 kV pulse of 2 μsec duration to alternate plates. A similar pulse of -20 kV was applied simultaneously to the remainder of the plates. This produced an intense electric field of about 10 kV/cm in the region of the gas in the tube. Electrons formed in the neon gas by the passage of the ionising particle undergo acceleration in the field, and acquire sufficient energy to initiate a Townsend discharge which fills the entire tube. To prevent the spread of discharge to adjacent tubes by photoionisation each tube was shielded from the other by black paper wrapping.

The main conclusions drawn from Conversi's experiments were that only tubes filled with spectroscopic neon and pulsed after very short time

delays ($< 2\,\mu$sec) could profitably be used.

III. 3. The Experiments of Barsanti et al.

Barsanti et al (1956), using the same equipment as Conversi et al have made more detailed measurements on the tubes particularly on the variation of layer efficiency with various parameters. The layer efficiency (η) is defined as the ratio of the number of single flashes observed in a layer to the number of single particles passing through the layer. The variation of efficiency with applied field strength (E), time delay (T_D) and pressure (p) of neon were studied and their results are shown in figures 2, 3, and 4.

Fig. 2 shows the variation of efficiency with the applied field for tubes filled with spectroscopic neon and a mixture of spectroscopic neon and 2% argon. The mixture gives a longer plateau 3 - 10 $kV/_{cm}$ and a lower threshold. The plateau is also found to be independent of the pulse length and rise time.

Fig. 3 shows the variation of efficiency with pressure of neon. The efficiency is seen to increase with increasing pressure reaching a maximum value of 0.75 at ~35 cm Hg after which there is a slight decrease.

The variation of efficiency with time delay is shown in fig. 4. It is seen that the efficiency falls off rapidly with increased time delay.

The main results of Barsanti et al may be summarised as follows:

(a) The efficiency increases with increasing value of the field strength and reaches a 'saturation' value.

(b) Argon lowers the threshold voltage and increases the length of the plateau

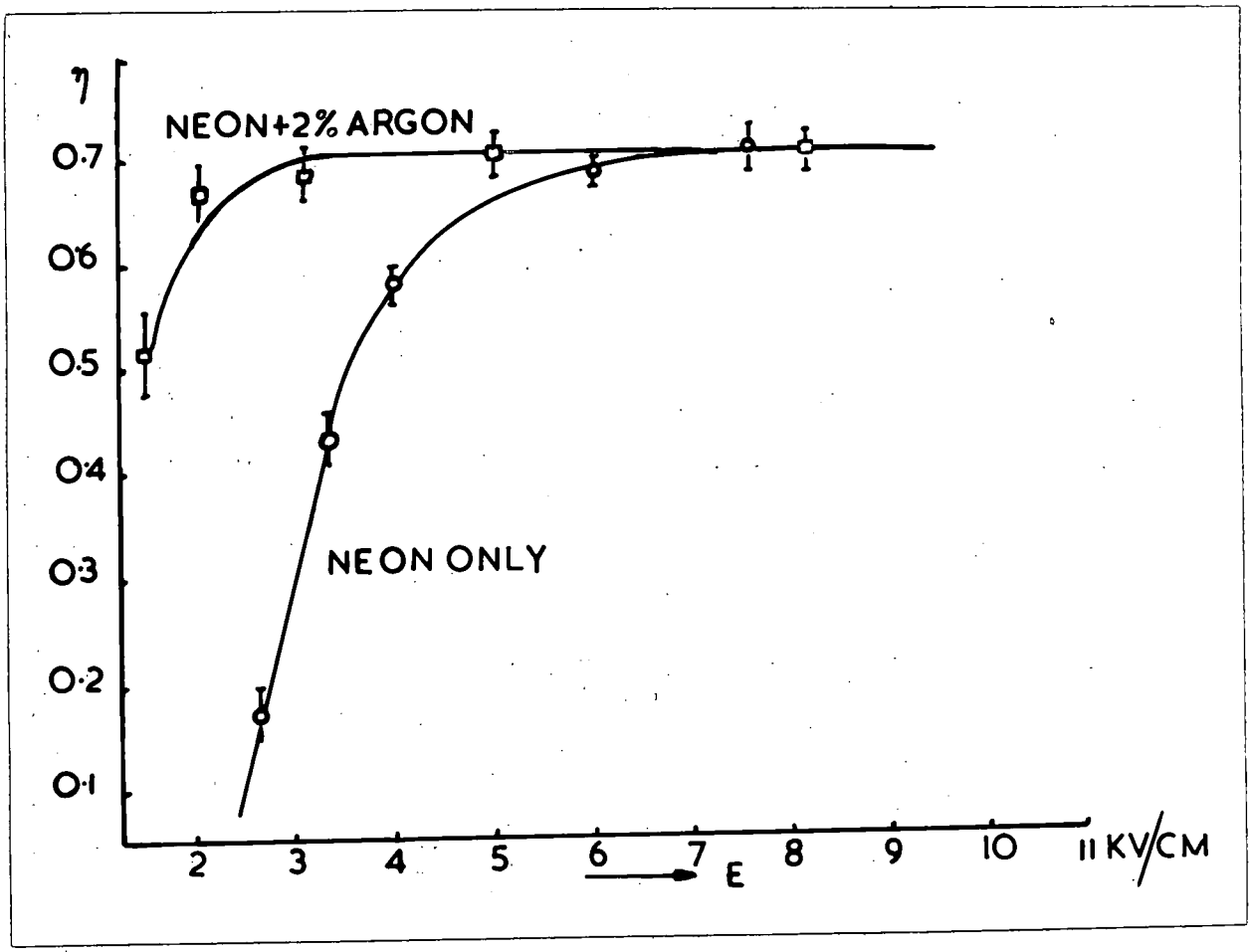

Fig. 2.

Variation of Layer Efficiency with Field

(Barsanti et al, 1956)

Pulse Characteristics

τ = 2.2 μ-sec

T_R = 0.15 μ-sec

T_d = 0.9 μ-sec

Max. Possible Layer Efficiency

= 82.5%

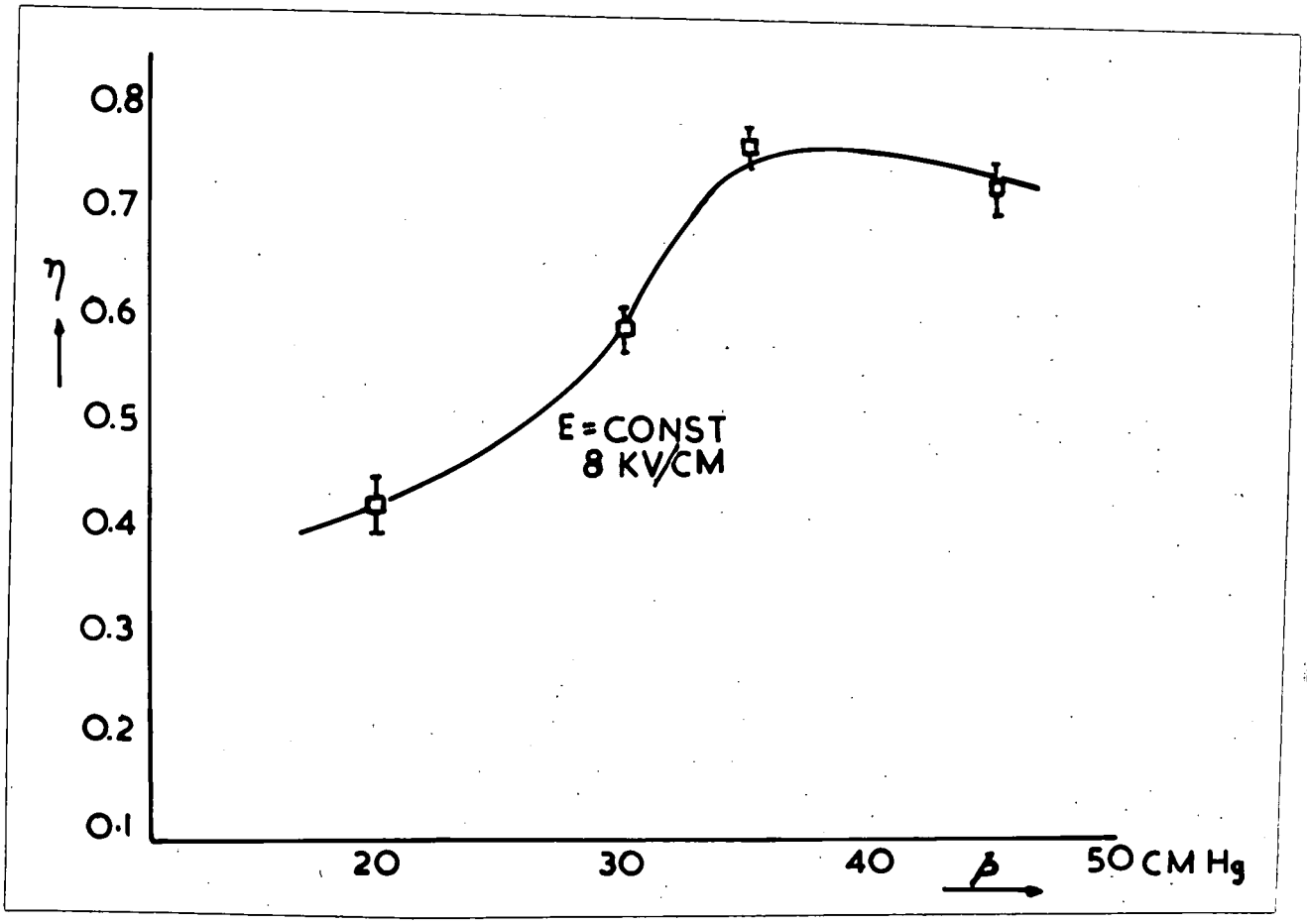

Fig. 3.

Variation of Maximum Efficiency with Pressure

(Barsanti et al, 1956)

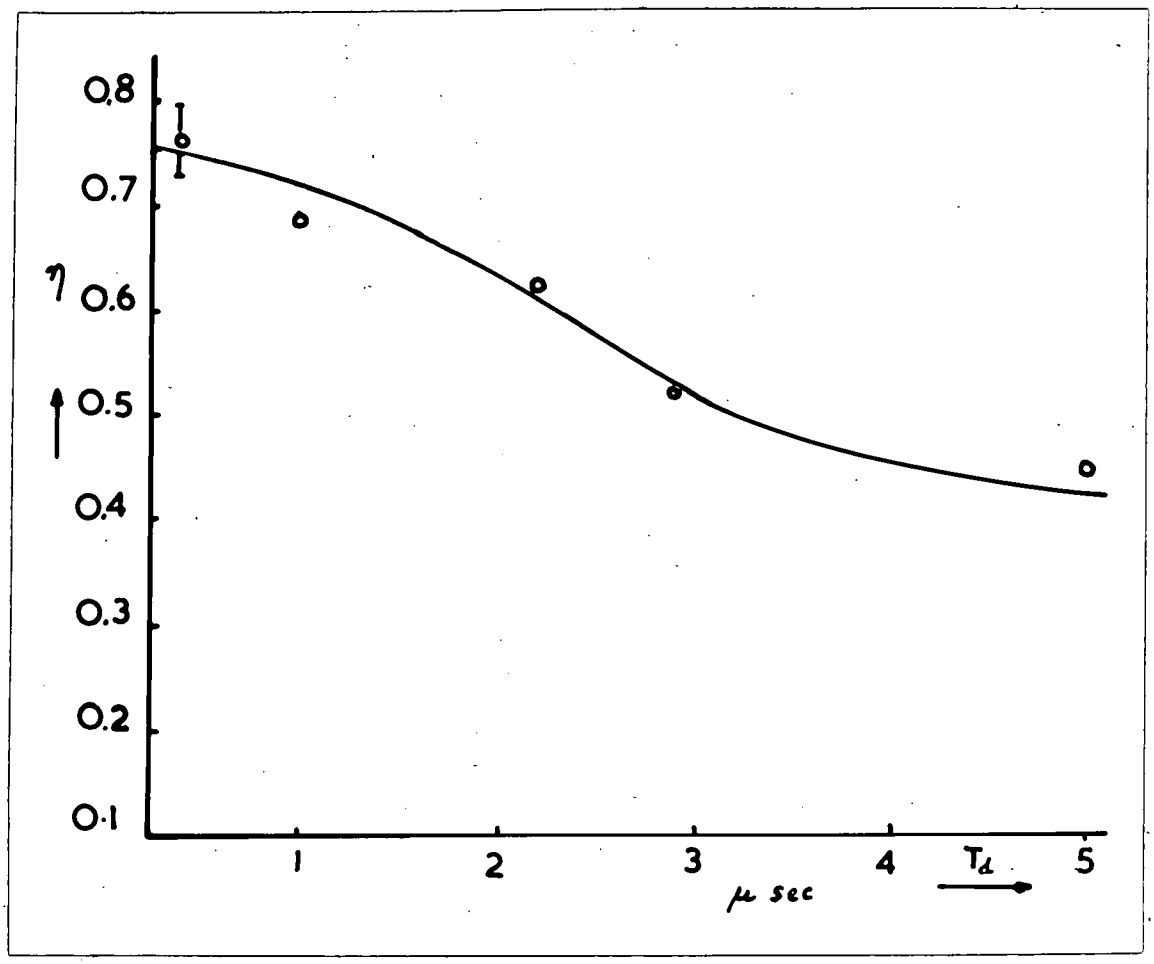

Fig. 4.

Variation of Efficiency with Time Delay

(Barsanti et al, 1956)

(c) There exists an optimum value of the pressure of neon for tubes of high efficiency.

(d) The efficiency falls off rapidly with increased time delay.

These workers reported that the efficiency of tubes filled with commercial neon was very low for time delays greater than ~0.3 μsec. Further, they found it necessary to evacuate the tubes to a pressure of 10^{-5} mm Hg before filling.

These characteristics are not satisfactory for the application envisaged here. The cost of the neon would be very great and since the time delays met with in the five-fold coincidence requirement of the spectrograph would be of the order of 7 μsec the effiency would be very low. As a result a systematic investigation of all the relevant parameters was carried out, with the particular object of designing a flash tube suitable for use in the spectrograph. Some theoretical analysis has also been attempted where it concerns aspects of practical importance.

CHAPTER IV

THE CONSTRUCTION OF NEON FLASH TUBES AND THEIR ASSOCIATED EQUIPMENT

IV. 1. The Filling System and Filling Procedure.

Since the range of filling conditions might be extensive a versatile vacuum system was required. The filling system is shown in fig. 5.

An oil diffusion pump assisted by a two stage Cenco-hyvac backing pump was used to evacuate the system down to pressures of 10^{-6} mm Hg. Liquid nitrogen traps were used to prevent mercury vapour entering the tube system. The ultimate pressure obtained in the system was measured by the McLeod gauge; the Pirani gauge was used in the early stages of filling to detect leaks in the system. The entire manifold was built into an oven in order to outgas the glass tubes by baking prior to filling. The spectroscopic gas was stored in glass flasks of one litre capacity. The commercial neon, contained in cylinders, was connected via a liquid nitrogen trap and a barometer.

Since the major portion of the system was constructed of Pyrex glass it was found possible to obtain a vacuum of 10^{-6} mm Hg within 30 minutes of switching on the heaters of the diffusion pump. With the commercial neon cylinder connected to the system it was found possible to obtain a vacuum of the order of 5.10^{-5} mm Hg.

The rate of leakage of gas into the filling system under exactly the same conditions of filling was determined prior to each filling. This value was usually of $\sim 10^{-5}$ mm Hg/min and under favourable conditions the tubes

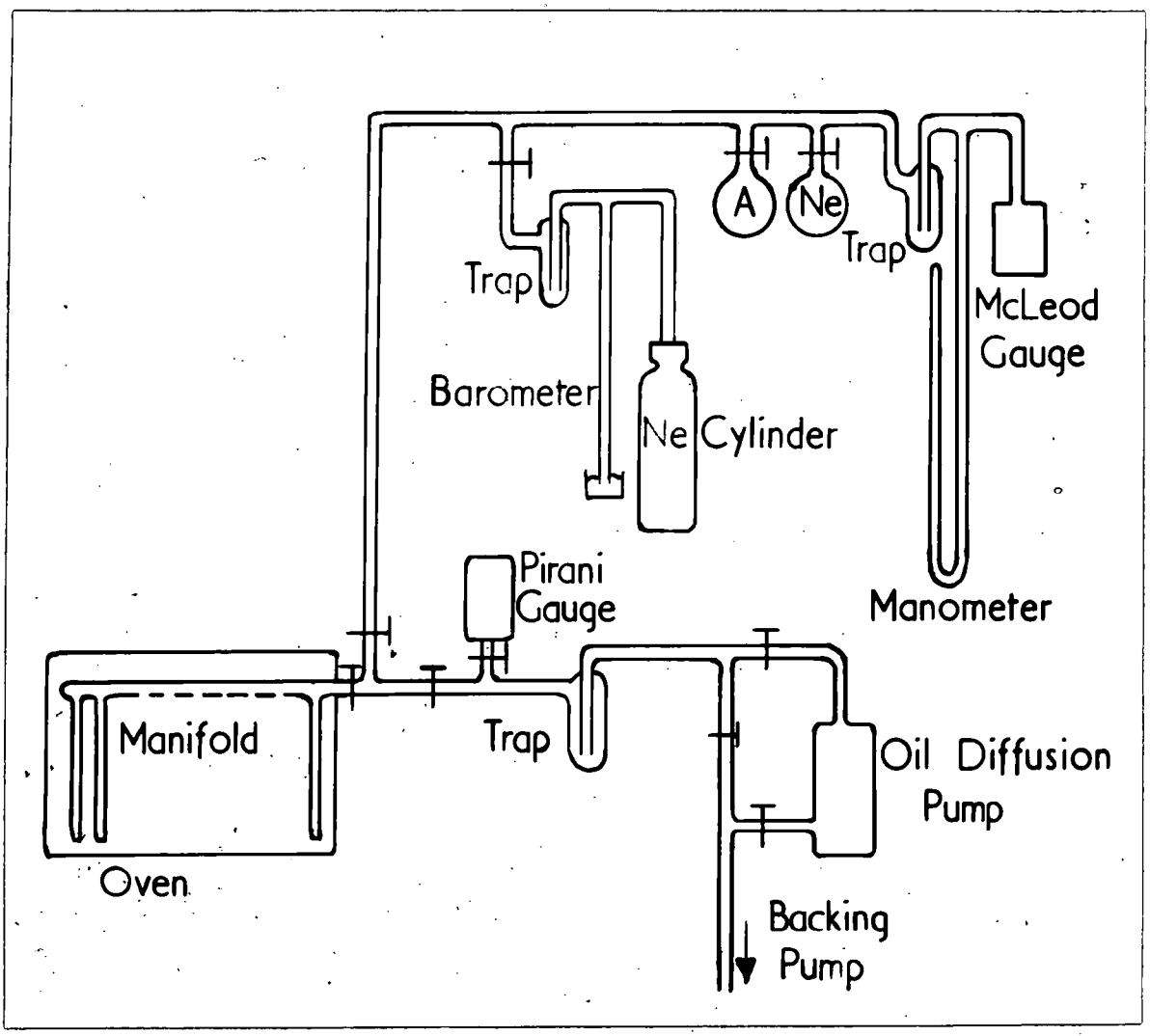

Fig. 5

The Filling System

could be filled to 65 cm Hg in less than half a minute. The pressure of neon in the tubes was measured directly by the Manometer.

The tubes were chemically cleaned in the usual manner by rinsing them with chromic acid, tap water and distilled water. After flattening one end they were sealed on to the manifold and evacuated. The tubes were then outgassed at 300°c for about 50 minutes and allowed to cool down to room temperature. The system was flushed out once or twice with the gas under investigation before filling the tubes at the desired pressure. Known amounts of spectroscopic argon or other 'impurities' could be introduced before filling them with the major constituent. After allowing some time for the gas to diffuse uniformly they were sealed off and painted with black cellulose paint.

IV. 2. The Experimental Arrangement

The apparatus shown in fig. 6 was used to determine the efficiencies of the tubes. Six tubes of the same filling were placed in a horizontal layer. Eight such layers formed the tube assembly. Thin aluminium plates were used as electrodes, alternate plates being connected together. The high voltage pulse was applied to one set and the other set was connected to earth.

IV. 3. The Electronic Circuits

The tube assembly was placed between a four-fold counter telescope A, B, C, D, shown in fig. 6, with the counting rate of 10 per minute. An ionising particle, on passing through the telescope, triggered a four-fold coincidence unit. This produced a positive pulse of 100 volts which was

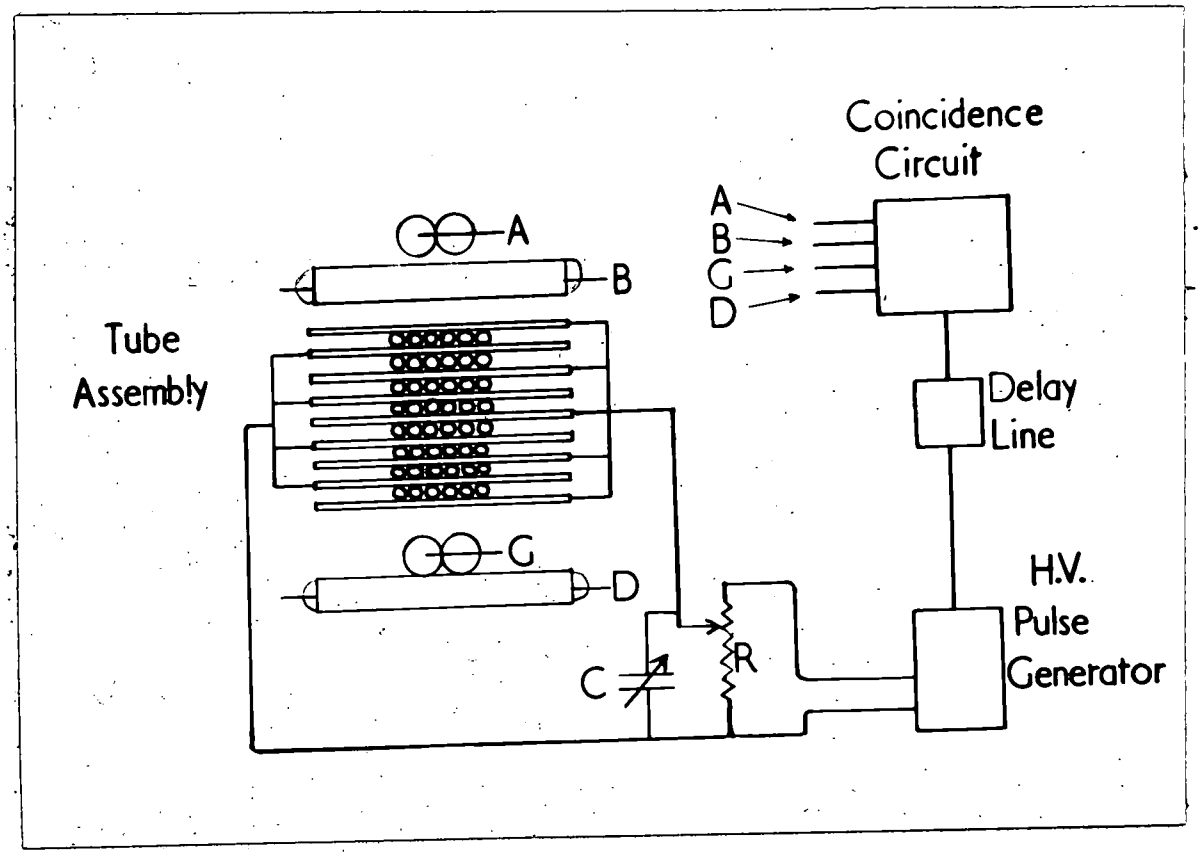

Fig 6.

Experimental Arrangement

delayed by a delay line and then fed into a high voltage pulse generator. The camera was also driven by a negative pulse from the same coincidence unit.

The high voltage pulse was produced in a manner similar to that described by Conversi et al. An open delay line was discharged through a thyratron (XH8) in series with the primary of a pulse transformer. The circuit used is shown in fig. 7. The coupling between the small thyratron (CV797) and XH8 was made by a coupling transformer using Ferrox-cubes (Mullard Limited) as the magnetic material to ensure a sharp pulse with a rise time of a fraction of a microsecond. The delay T_D between the passage of the particle and the application of the pulse was controlled by a delay line shown in the figure . Variations in the height of the pulse applied to the plates were effected by adjusting the tapping on the matching resistor R. The rise time T_R could be adjusted by changing the capacity of a high voltage condenser C. Different values of the pulse width τ were obtained by varying the number of sections used in the pulse forming network. A typical pulse is shown in Fig. 9. τ is the pulse width at 75% of the peak height and T_R the rise time to reach the same height.

The choice of values for the variables T_D and T_R was made bearing in mind the values likely to be attained in the practical application of the technique. For investigations involving a number of layers of Geiger counters several meters apart connected in coincidence to control the operations of the flash tubes, delays of several (7 to 8) microseconds between the passage of the particle and the generation of the coincidence

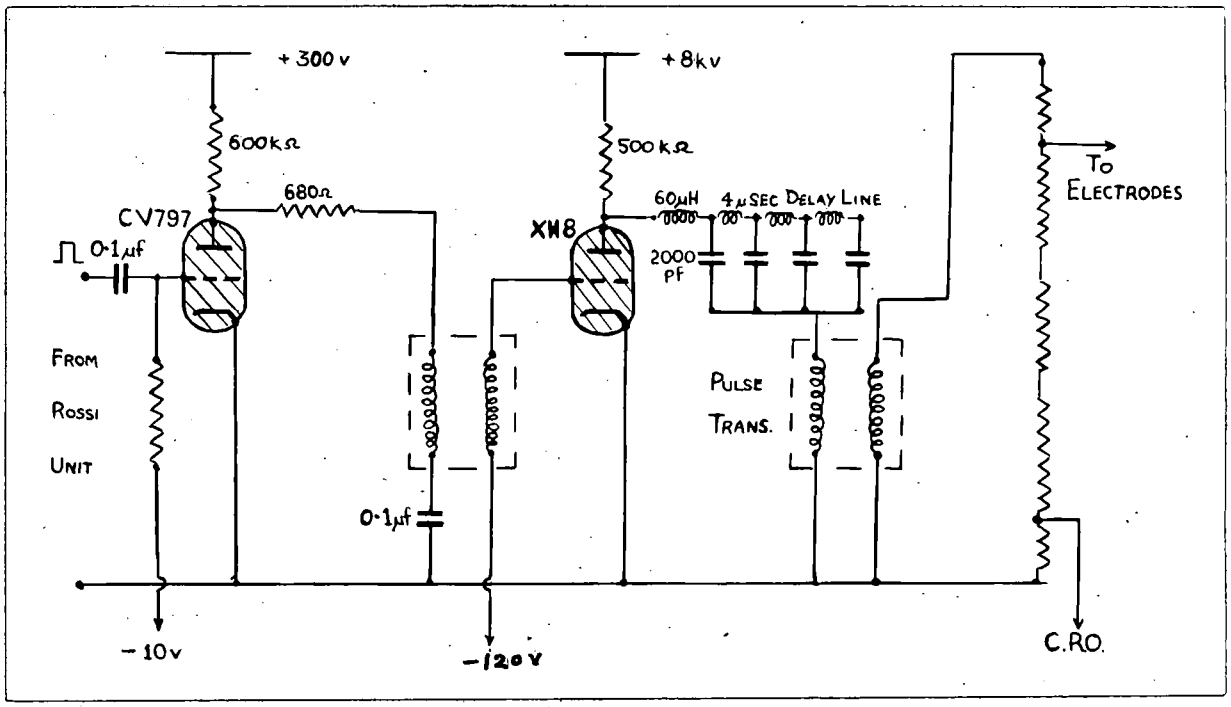

Fig. 7

The High Voltage Pulse Generator.

pulse may occur. In addition, a relatively large value of T_R is often dictated by the necessity of applying the high voltage pulse to a large array of tubes having considerable electrostatic capacity.

CHAPTER V

THE CHARACTERISTICS OF LOW PRESSURE TUBES

V.1. The Characteristics under Investigation

The basic requirements of the tubes are that they should have a high efficiency for flashing when a particle passes through the array within the resolving time of the apparatus (a few μsec) and small number of spurious flashes, i.e. flashes not due to the passage of a particle. Two efficiencies may be defined, firstly the layer efficiency (η see chapter III.3) and secondly, the absolute efficiency, defined as the ratio of the number of observed flashes to the number of particles passing through the gas in the tube. These efficiencies are a function of a number of parameters, for example, the dimensions, the glass, the pressure of the main constituent of gas filling and the pressures of the contaminants added intentionally or unavoidably present and finally the characteristics of the high voltage pulse.

The optimum diameter of the tube is found to be in the region of 5-7 mm. This value gives a high enough maximum layer efficiency and a reasonably small number of layers is necessary to give the required spatial resolution. The types of glass investigated were those commonly encountered viz. Pyrex and Soda. Most of the measurements were made on Pyrex tubes 7.85 mm external diameter 5.75 mm internal diameter and Soda glass tubes of 7.28 mm external and 5.58 mm internal diameter. The main constituent of the gas used in the tubes was either spectroscopic or commercial neon. An estimate of the constituents of the two grades of neon is given in Table 1. (British Oxygen Co. specification).

TABLE I

Constituents of the Gas

Gas	Spectroscopic neon (NeS)	Commercial neon (NeC)
Neon	99.9%	98%
Helium	$\leqslant$ 1 v.p.m.	2%
Nitrogen	1 v.p.m.	100 - 200 v.p.m.
Oxygen	$\sim$1 v.p.m.	$\leqslant$ 10 v.p.m.
Hydrogen	$\sim$1 v.p.m.	$\leqslant$ 10 v.p.m.

(v.p.m. = volumes per million)

V. 2. Experiments with Pyrex Glass Tubes.

Prompted by the comparative ease of working with Pyrex glass 50 tubes were filled with commercial neon to a pressure of 65 cm Hg and tested for spurious flashes by applying random pulses to the plates. These were obtained from a pulse simulator which gave 10 pulses per minute. It was found that at field strengths above 6kV/cm most of the tubes flashed spuriously. The assembly of the tubes was then subjected to 'genuine' pulses from the four-fold coincidence unit. This time the applied pulses were such as to give field strengths of $\sim$6 kV/cm. The tubes were found to have zero efficiency. A similar experiment was performed with tubes made of Soda glass and filled with commercial neon to the same pressure.

Of the 50 tubes tested only 5 % flashed spuriously below 12 kV/cm; these were rejected. Of the remainder 5% flashed spuriously in the region 12 - 15 kV/cm.

This difference in behaviour is perhaps due to the different electrical properties of the glass. The volume specific resistance of Pyrex is 10^{15} ohm cm compared with 10^{13} ohm cm for Soda. Pyrex glass has a surface resistivity 10^{9} ohms and Soda 10^{6} ohms. The value of the latter quantity depends on the presence of layers of impurity on the surface.

One explanation of the spurious flashing is then as follows: electrons from earlier ionisation by cosmic rays or natural radio-activity stick to the walls of the tube. These should take a longer time to leak away in Pyrex than in Soda glass tubes due to their difference in surface and volume resistivities. Thus, spurious flashes might be expected to be more frequent in Pyrex glass since there will be more detachable electrons on the surface of tubes made of this glass.

Since tubes made of Pyrex glass proved unsuitable, all subsequent measurements were made on Soda glass tubes.

V. 3. Reproducibility of Tube Characteristics

To find how accurately the conditions of filling could be reproduced the efficiencies of two batches of tubes, filled with commercial neon to a pressure of 65 cm Hg under very similar conditions, were measured. Fig. 8 shows the variation of efficiency with field strength for these batches. It will be noticed that although the shapes of the curves are similar, one is higher by nearly 9%. This lack of reproducibility should be borne in mind

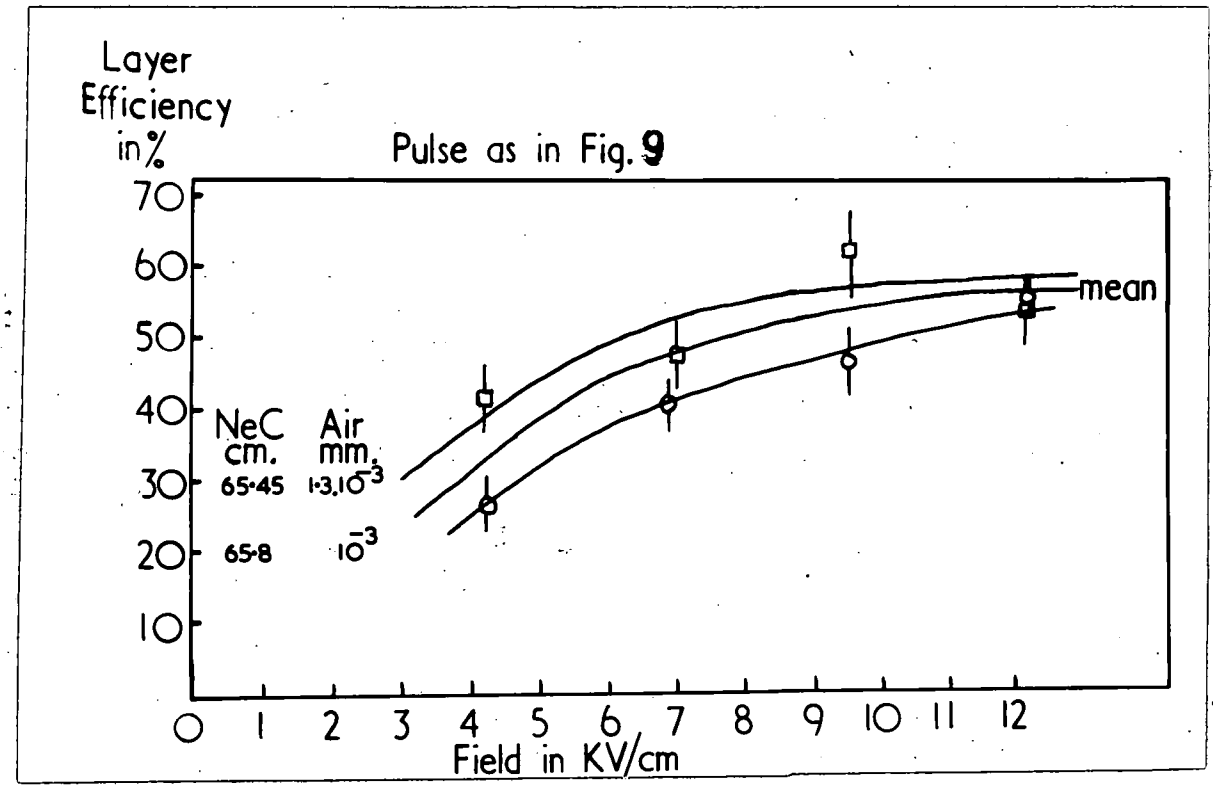

Fig 8.

Characteristics of Tubes Filled under Similar Conditions.

when detailed comparisons are made.

The errors in the experimental points are obtained from an expression derived in the Appendix.

V.4. The Variation of Efficiency with Residual Air Pressure

Investigations were carried out with tubes filled with 65 cm Hg commercial neon at a residual air pressure ranging from 10^{-5} mm Hg to 1 mm Hg. The variation of efficiency with field strength for various air pressures is shown in fig. 9, together with the characteristics of the high voltage pulse. Examination of the curves shows that the effect of the presence of increasing amounts of air is two-fold. Firstly, it reduces, the maximum efficiency of the tubes at field strengths of 12 kV/cm and secondly it lowers the threshold voltage for high efficiency of flashing. It is interesting to note that with tubes containing 1 mm of air the efficiency at field strengths of 4 kV/cm is 55% compared with 15% for tubes containing 10^{-5} mm Hg of air.

The reduction in the maximum efficiency of the tubes is undoubtedly due to the presence of oxygen. It is known that electrons become attached to oxygen molecules and can thus be effectively removed from the sensitive volume by the time the pulse is applied.

The presence of the small amount of argon (.9%) present in air could explain the reduction in the threshold for high efficiency of flashing. (See V.6).

V.5. The Variation of Efficiency with Pressure of Neon.

The maximum efficiencies at field strengths of 12.2 kV/cm are given as a function of pressure in fig. 10.

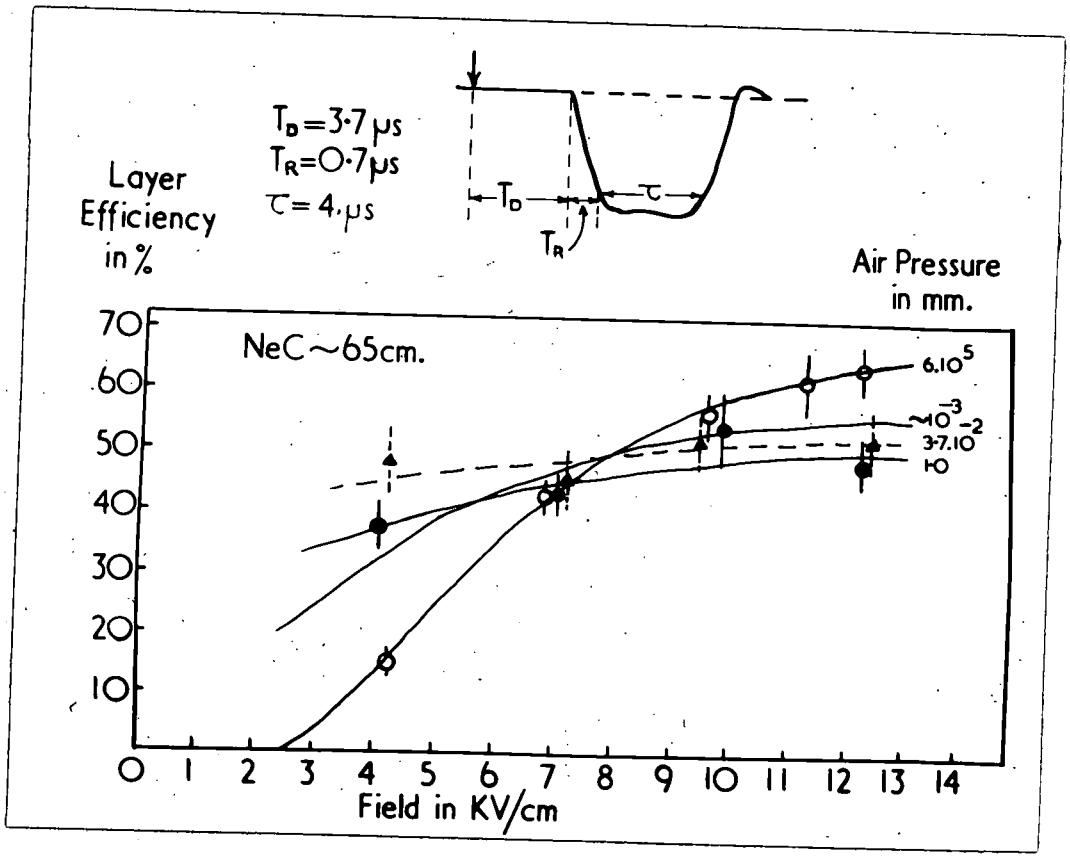

Fig. 9

Variation of Efficiency with Residual Air Pressure

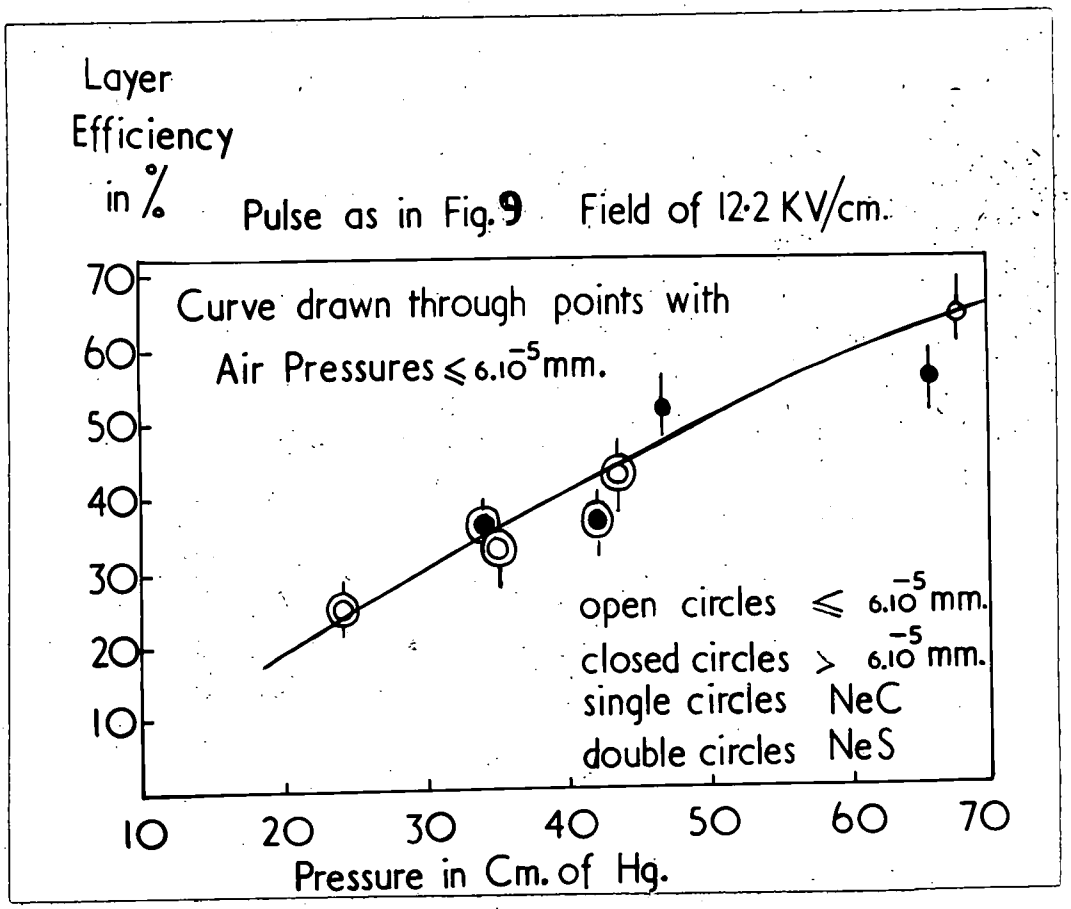

Fig. 10

Variation of Efficiency with Pressure.

No marked differences are apparent between the efficiencies of the tubes filled with commercial or spectroscopic neon in the region of overlap 40 cm Hg. The observed efficiencies are found to fit on a smooth curve. It is also seen that there is a steady increase in efficiency with pressure of gas. This increase in efficiency may be explained as due to the increase with pressure in the number of primary ion pairs produced by the ionising particle in the gas, thus compensating and outweighing the loss of electrons by various mechanisms.

V.6. The Variation of Efficiency with Pressure of Argon.

It is known that the presence of a small percentage of argon has a profound effect on gas discharges in neon. Experiments were therefore performed with various admixtures of argon. Twenty tubes were evacuated to an ultimate pressure of 10^{-5} mm Hg and filled with commercial argon to a pressure of 10^{-2} mm Hg before filling with commercial neon to a pressure of 65 cm Hg. Efficiency measurements carried out on these tubes yielded very low values (15%). It was therefore decided to use spectroscopic argon as the contaminant.

Tubes filled with the usual pressure of neon and spectroscopic argon up to a pressure of 6 mm Hg were found to possess efficiencies as high as 50% even at the low field strength of 4 kV/cm. The result of the efficiency measurements on the various batches of tubes is shown in fig. 11. It is seen from the curves that the efficiency of the tubes at field strengths 11 - 15 kV/cm is highest for tubes containing commercial neon only and the efficiency of tubes at low values of field strengths of $\sim$ 4 kV/cm is highest for tubes containing argon at a pressure of $1.5.10^{-2}$ mm Hg (i.e. a

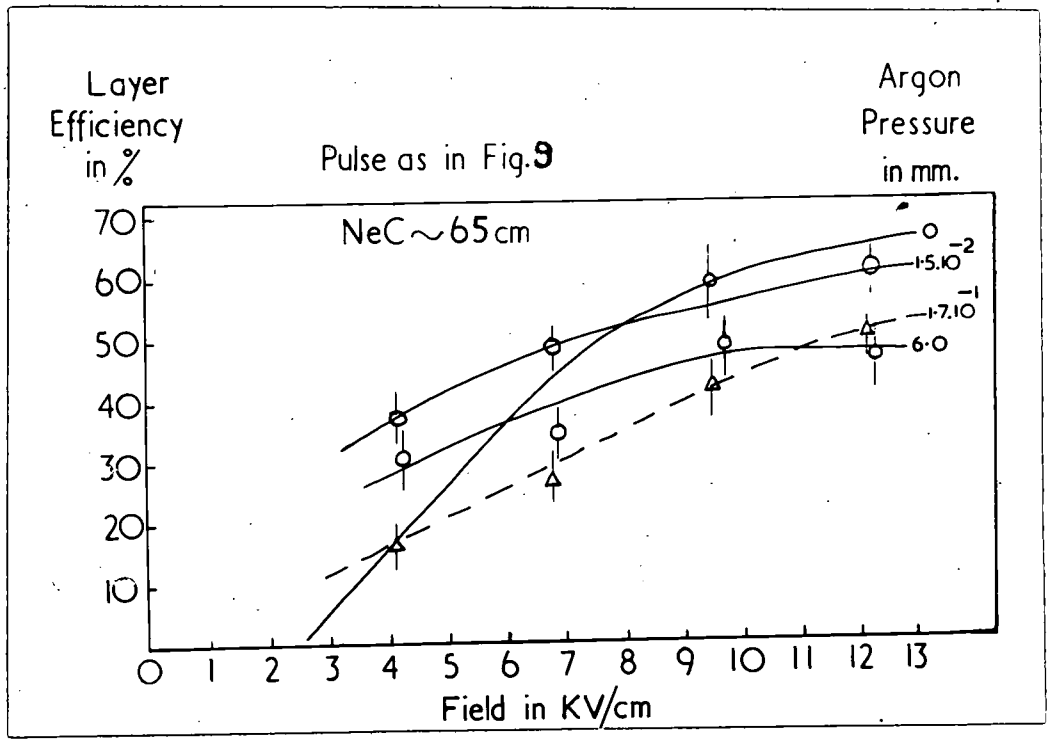

Fig. 11.

Variation of Efficiency with Field for Various Pressures of Argon.

fraction of $2.5.10^{-5}$%). Furthermore, there exists an optimum argon pressure at which the efficiency is a maximum. The increase in efficiency of tubes containing argon at low field strengths may be attributed to the increase in the total specific ionisation produced in the mixture of the gas by the incident particle and the increase in the value of the ionisation coefficient η_o (η_o is the probability of ionisation by an electron per volt potential difference). The first of these two effects has been studied by Jesse and Sadauskie (1952) who measured the number of ion pairs produced by an α- particle (5.29 M.e.V) from polonium in an ionisation chamber containing successively pure neon and mixtures of neon and argon. They found that with pure neon the number of ion pairs per polonium α-particle was ~146,000, whereas for a mixture of neon + 0.12% argon the number rose to 203,000. This effect was attributed to the presence of metastable states in neon. Excitation of neutral neon atoms (Ne) often brings them into a metastable state (Ne*) of high energy eV_m and long life-time. The argon atom (A) has an ionisation potential $V_i < V_m$. Thus the metastable atoms of the main gas are able to ionise the atoms of argon in the following manner:

$$Ne^* + A \longrightarrow Ne + A^+ + e^-$$

The cross-section for this process is large enough for small amounts of argon to cause a considerable increase in the total ionisation produced by the charged particle.

The variation of η_o with increasing amounts of argon in a neon-argon mixture has been summarised by Druvestyn and Penning (1940) as shown in

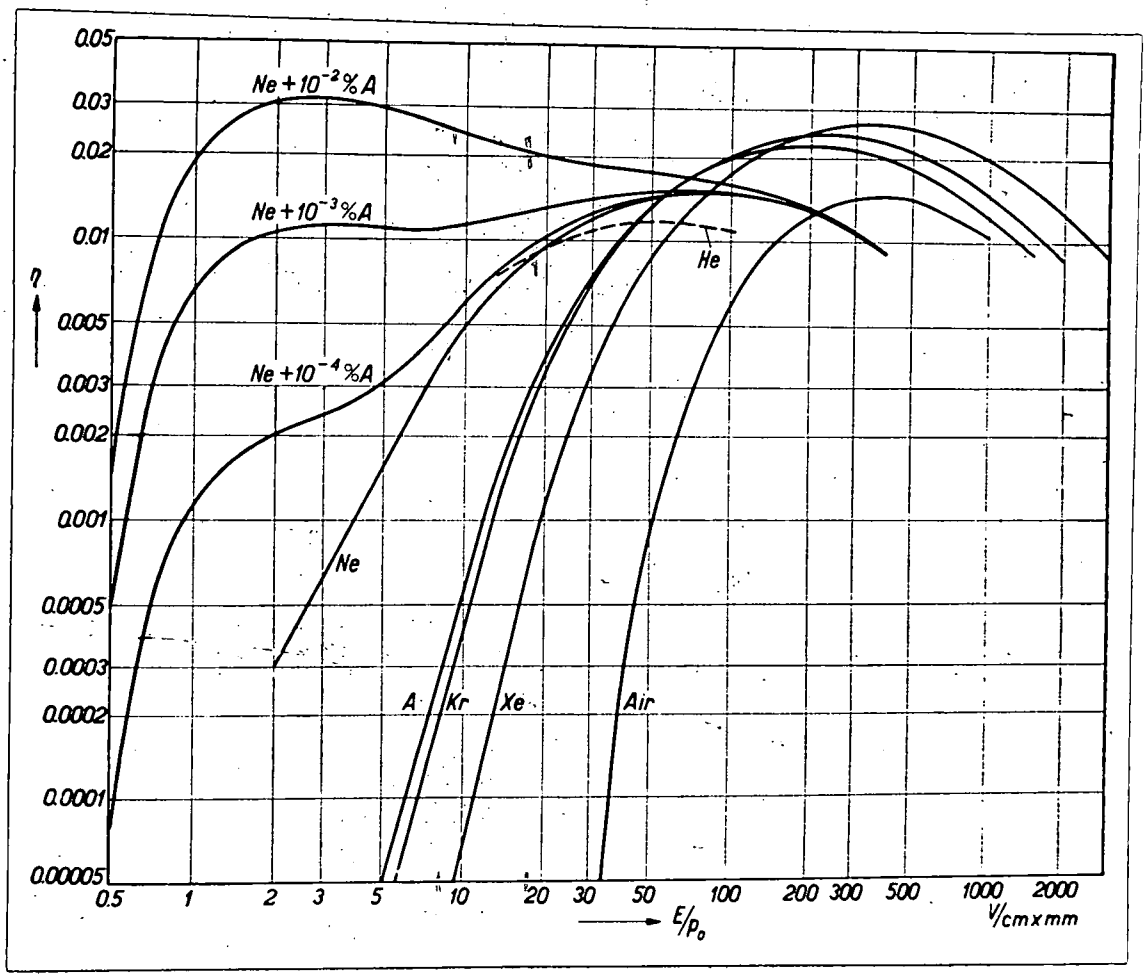

Fig. 12

The Variation of Ionisation Coefficient η_0 with E/p_0 for various Gases and Gas Mixtures. The Field E is measured in volts/cm and the Pressure p_0, in mm.Hg. (After Druyvestyn and Penning, 1940).

fig. 12. It is seen that for an argon content of 10^{-2}% the value of η_0 for field strengths of 12kv/cm is increased by a factor of three over the value for pure neon. At field strengths of 6 kv/cm the value of η_0 is increased by a factor of seven over that for pure neon. This increase in the efficiency is again attributed to the presence of metastable states in neon. In the absence of argon atoms an electron requires an energy of 21.5 ev (ionisation potential of neon) to produce further electrons by ionising atoms of neon. In an argon-neon mixture, however, the excited metastable states (16.55 and 16.62 e.v.) have enough energy to ionise an argon atom (15.8 e.v.ionisation potential) by collision.

As stated earlier it has been noticed that the efficiency of tubes at field strengths of 11 - 13 kv/cm is highest for tubes containing commercial neon only. This result is contrary to expectation and is inconsistent with the results of Conversi et al, who found that the maximum efficiency did not vary with the percentage of argon. It is possible that the discrepancy is not real but arises from the lack of reproducibility referred to before. Further experimental study is necessary before this anomalous variation can be explained.

The increase in efficiency at low field strengths in the case of tubes filled with neon and air can now be understood. Itis known that air contains about 0.9% argon. This could therefore be responsible for the increase in efficiency of tubes at low field strengths for tubes filled with neon and air.

Whether there is a reduction of maximum efficiency when argon is

present or not there is little to be gained by adding argon to the gas filling for the following reason. The intensity of the flash at low fields, where the efficiency of the tubes containing argon is higher, is in general too low for good photographic records to be taken.

V. 7. (a) The Variation of Efficiency with Time Delay.

A study of the variation of efficiency with time delay is necessary for two reasons: (a) the sensitive time of the tube and the consequent probability of a flash not being due to the triggering particle is determined by this variation, and (b) in operation the efficiency must not fall appreciably by the time the high voltage pulse is applied. This variation has been determined for tubes having a wide variety of fillings. The constituents of the different batches of the tubes are given in Table II. ~~All the tubes were filled with commercial neon to a pressure of 65 cm Hg.~~

TABLE II

Pressure of neon cm Hg	Pressure of contaminant mm Hg	Reference number
66.5 NeC	0.17 argon	1
67.1 NeC	1.0 air	2
66.5 NeC	6×10^{-5} air	3
65.5 NeC	1.3×10^{-3} air	4
66.8 NeC	1.5×10^{-2} argon	5
46.1 NeC	3.0×10^{-4} air	6
43.6 NeS	$< 10^{-5}$ air	7
34.0 NeS	5.10^{-4} air	8

The delays chosen in the experiment were greater than 4 μsec since this was the shortest possible delay expected in the spectrograph. The pulse height was chosen to give a field strength of 11 kv/cm, the pulse width being 4 μsec. The results of the measurement are shown in fig. 13. Comparison of the curves 3, 4 2 filled with commercial neon to 65 cm Hg at various residual air pressures show the increasing rate of fall of efficiency with time delay for tubes with increasing amounts of air. The effect of reducing the pressure of neon can be seen by comparing the characteristics of curves 4 and 6. At the lower pressure the fall of efficiency is more rapid.

V.7. (b) Theoretical Analysis.

In the interval between the passage of the ionising particle through the tube and the commencement of the avalanche, several mechanisms are responsible for reducing the number of electrons available to initiate the avalanche. The more important of these are (i) recombination (ii) diffusion of electrons to the glass walls and (iii) capture and attachment to neutral atoms to form negative ions of low mobility. The contribution made by each of these to the variation in efficiency with time delay will be discussed in turn.

(i) Recombination: If the numbers of positive and negative ions per cm^3 are n_+ and n_- respectively, the number of recombinations per second is

$$N = \alpha_r n_+ n_- \quad \ldots\ldots\ldots\ldots\ldots \quad (1)$$

where α_r is the co-efficient of volume recombination and is 2.10^{-7}

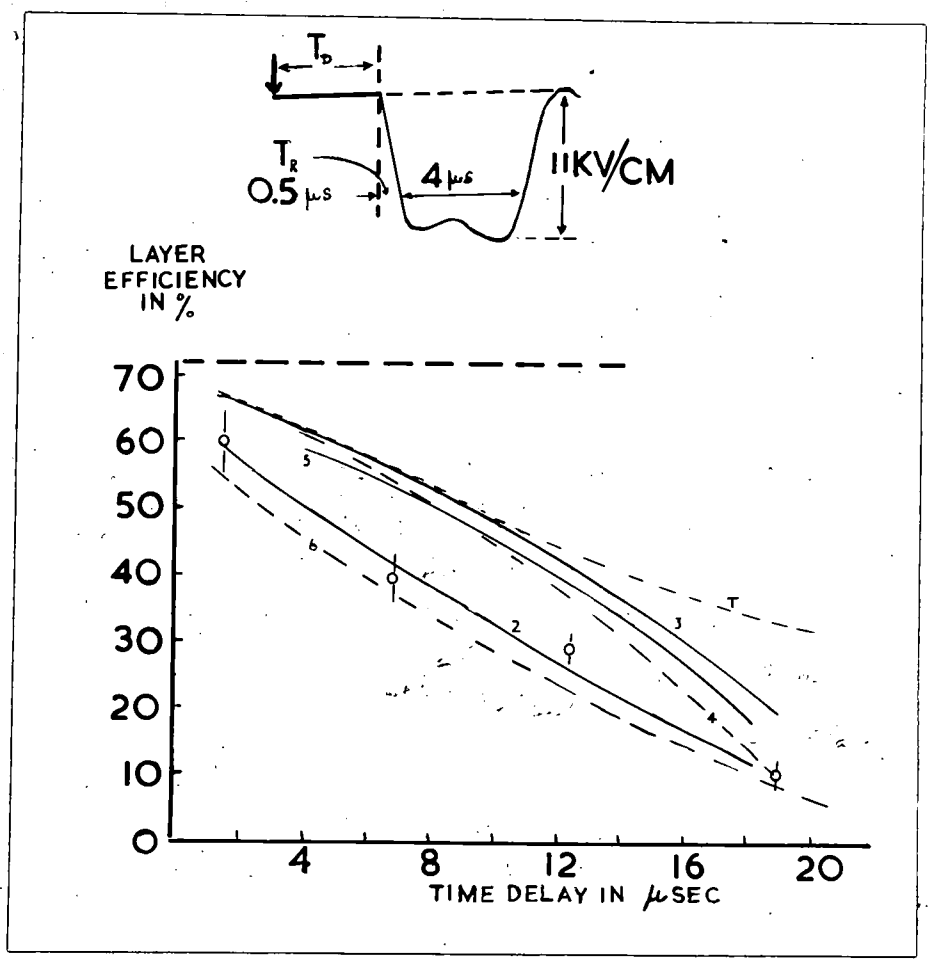

Fig. 13

Variation of Efficiency with Time Delay.

cm ion^{-1} sec^{-1} for neon (Biondi and Brown 1949). It is known that n_+ and n_- for a track at near minimum ionisation in neon at 65 cm Hg are each of the order of 20 ions cm^{-3}. It is thus apparent from equation (1) that the contribution to the electron removal by volume recombination is negligible.

Preferential recombination , i.e. recombination of the original members of the ion pair, will be more important but even this effect should be small since the free electrons produced in the ionisation process have appreciable energy and soon escape from the neighbourhood of the positive ions.

(ii) Diffusion of electrons to the glass wall.

In the interval between the passage of the particle and the application of the pulse the electrons in the gas slowly diffuse to the walls where it is assumed they stick and do not contribute to the production of the avalanche. Assuming that all the electrons produced by the particle at time t = o are at the centre of the tube, the number N_t remaining in the tube after time $t = T_D$ can be calculated.

If No ions are concentrated at the origin at t = o then after time t, the number between x and x+ dx is

$$N_x\,dx = \frac{N_0}{(4\pi D t)^{\frac{1}{2}}}\ exp\left(-\frac{x^2}{4Dt}\right)dx$$

where D is the diffusion coefficient. It is easily shown that the corresponding number in an elementary annular ring is

$$\frac{N_0 r}{2Dt}\ exp\left(-\frac{r^2}{4Dt}\right)dr$$

Thus the probability dP of finding an electron in this area is

$$dP = \frac{r}{2Dt}\, e^{-\frac{r^2}{4Dt}}\, dr$$

For a tube of radius R having an electron at its centre at time t = o the probability of the electron still being in the tube after t seconds is given by

$$P = \int_0^R e^{-\frac{r^2}{4Dt}}\, d\left(\frac{r^2}{4Dt}\right) = 1 - e^{-\frac{R^2}{4Dt}}$$

Taking the following values, R = 0.28 cm, D = $8.4.10^3$ cm^2/ sec, and t = 5.10^{-6} sec, for a typical flash tube, the value of the probability is found to be o.373.

If the production is assumed to take place not at the centre but along a diameter then equation (1) may be written

$$P = \left(1 - exp - \frac{R^2}{4Dt}\right) f\left(\frac{R^2}{4Dt}\right)$$

where $f\left(\frac{R^2}{4Dt}\right)$ is a geometrical function.

In actual fact the electrons are produced along paths of various lengths. This can be allowed for to a first approximation by using for N_o the number electrons produced on the mean path length $\bar{L}$. This number must be reduced still further, however, because electrons produced near the wall might not be expected to initiate an avalanche on acceleration. (Conversi et al 1955). If the effective insensitive depth of the counter is written as δ then the internal efficiency of a tube for recording an ionising particle is approximately

$$\eta(t) = \eta(o) \left[1 - \exp \left\{ - N_t \left(1 - \frac{\delta}{\bar{L}} \right) \right\} \right] \quad \ldots\ldots\ldots (2)$$

where $\eta(o)$ the efficiency at zero time delay is given by

$$\eta(o) = 1 - \exp \left[- n \left(1 - \frac{\delta}{\bar{L}} \right) \right] \quad \ldots\ldots\ldots (3)$$

and is the probability of at least one ion pair being present in the sensitive volume. n is the average number of primary ion pairs produced along the mean path length, δ is found by extrapolating the experimental curve (η , T_D) back to $T_D = 0$ and then using equation (2). The value of $\bar{L}$ chosen is such that $(\bar{L})^2$ is equal to the internal cross sectional area of the tube. The value of δ so found is 1.4 mm.

The theoretical curve has been evaluated by Gardener (1957) for the tubes filled with NeC at 65 cm Hg at a residual air pressure of 6.10^{-5} mm Hg. The total ionisation has been derived from the work of Jesse and Sadauskis (1952) who found that about 26.2 e.v. of energy are required to liberate an ion pair in neon, and the data of Eyeions et al (1955) which gave the most probable total energy liberated in the form of ionisation in neon. At a mean momentum of 1.G.e.V/c the most probable total specific ionisation in neon at 65 cm Hg pressure is about 21 ion pairs per cm. Fig. 13 shows the theoretical curve, marked T. It is seen that this agrees fairly well with the experimental curve for delays up to 10 μsec. Above this value the divergence becomes increasingly marked. The Einstein theory of diffusion should predict too high a value for the concentration of the electrons in the tube as it includes electrons which have diffused past the boundary and have then diffused back again. (Lloyd (1958) has

worked out the problem rigorously using the equation for the analogous problem of heat conduction. He finds good agreement between experiment and theory over a wide range of pressures after determining the diffusion coefficient from the observed variation at one pressure only

(iii) Electron Attachment.

The presence of gases having high electron attachment probabilities are responsible to a small extent for the removal of electrons. Electrons produced by the ionising particle may attach themselves to neutral atoms to form negative ions of low mobility. The most common impurity introduced intentionally was oxygen. In this case the electron attachment coefficient h at thermal energies is $\sim 2.5.10^{-4}$ Further, it is known that as the electron energy is increased h falls to a minimum at about 1.3 e.v. then rises to a maximum of $5.5.10^{-4}$ at 2 e.v. (Healey and Kirkpatrick, quoted by Healey and Reed, 1941). After a delay of 10 μ-sec the number of electrons attached to oxygen molecules in a tube containing 1 mm of air is about 10%. A qualitative explanation of fig. 13 is thus possible. The fall of efficiency with time delay is more rapid for tubes containing air where the attachment is important and for tubes filled at low gas pressures where h is comparatively low. It is interesting to note that with a time delay of 2 μ-sec the efficiency of the tubes containing 1 mm of air is virtually as high as that for those with an air pressure less than 10^{-5} mm Hg.

V. 8. The variation of Efficiency with Rise Time

The electrostatic capacity of the tube assembly has a marked influence on the rise time of the pulse. Values of capacity of 1000 p.f.s. were found to increase the rise time by about 2 μsec. Since the array of tubes to be used in the big spectrograph has a capacity of this order it was decided to investigate the variation of efficiency with rise time.

The various batches of tubes marked 1-8 (see Table II) were tested for their variation of efficiency with rise time of the pulse. The results and the characteristics of the applied pulse are shown in fig. 14. Examination of the curves 3, 4, 2 for tubes filled with commercial neon at 66.5 cm Hg and residual air pressures of $6.0.10^{-5}$, $1.3.10^{-3}$ and 1 mm Hg respectively shows that with increasing rise time the efficiency decreases. The rate of decrease of efficiency with rise time is greatest for tubes containing the highest percentage of air. This is due to the increased probability of electron attachment during the rise time of the pulse as the electron attachment coefficient has a resonance for electrons in the region of 2 e.v.

The reason for the lowering of efficiency with increasing rise time may be seen from the following approximate analysis. If w is the drift velocity produced by the field E, then over a wide range of field strengths the drift velocity is given by

$$w = k E \quad \ldots\ldots\ldots\ldots\ldots\ldots \quad (4)$$

where k is a constant $\sim 2.10^{6}$ for E in kv/cm and w is in cm sec^{-1}.

If the leading edge of the pulse is given by $E = \alpha t$ where α is a constant

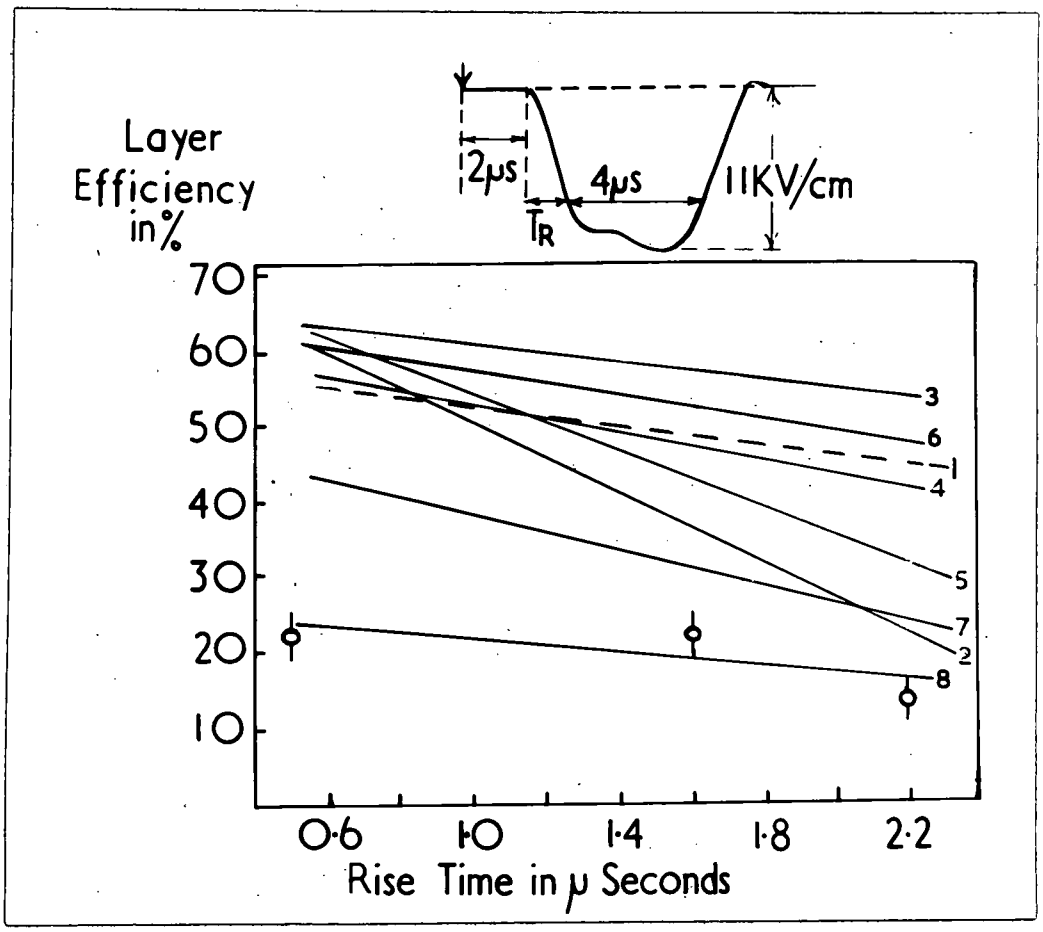

Fig. 14

Variation of Efficiency with Rise Time.

then the time taken for the electron to drift to a distance s is given by

$$t = \left(\frac{2s}{k\alpha}\right)^{\frac{1}{2}} \quad \ldots\ldots\ldots\ldots\ldots\ldots \quad (5)$$

For the maximum field strength of 11 kv/cm, rise time of 2 μsec and tube radius 0.28 cm we find $\alpha = 4.1 \times 10^6$. Using this value of α in equation (5) we have $t = 0.26$ μsec. In this time the applied field rises to 1.1 kv/cm. It is known that the variation of mean excitation energy ϵ with E for pure neon is such that ϵ increases up to a plateau of 12 e.v. at field strength of 3.0 kv/cm (Rossi and Staub 1949). At a field strength of 1.1 kv/cm, $\epsilon \sim 9$ e.v. This value is significantly below the maximum value and the number of electrons with energy above the ionisation potential (21.6 e.v.) can be expected to be considerably reduced. Therefore some reduction in efficiency is expected for the value of T_R considered (2 μ-sec).

V.9. The Variation of Efficiency with Pulse Length

The efficiency of the tubes was studied for two values of pulse length: 2 and 4 μsec. No difference was found for the tubes filled at lower pressures. A reduction would be expected when the pulse length is shorter than the time taken for the electron to traverse the tube. This time may be calculated using the drift velocity of the electron at field strength of 11 kv/cm. For a tube of diameter 0.58 cm the time taken is ~ 0.05 μsec. This assumes a square pulse. For a pulse with $T_R = 2$ μsec the time taken is ~ 0.4 μsec. Consequently no appreciable variation would be expected for pulse lengths in the region 2 - 4 μsec since these are in excess of

this value.

V.10. After-flashing.

If a flash tube is subjected to a second pulse a short time after the initial flash has occurred there is a finite probability of the tube flashing again. This phenomenon was studied quantitatively in the following manner. The tubes which flashed at the passage of an ionising particle through the assembly were noted. After a short interval of time the assembly was subjected to a similar high voltage pulse. Then tubes that flashed for a second time were noted. This procedure was repeated for several hundred particles. The time interval between the application of the first and second pulse was varied from 0.5 to 10.0 seconds. The probability of flashing as a function of time intervals is given in fig. 15. It is noticed that tubes filled with commercial neon at high pressures have a 'dead time' of about 10 seconds whereas tubes containing mixtures have shorter dead time of the order of 1 sec.

The reason for the phenomenon of after flashing is that considerable time is taken for the very large number of electrons produced in the avalanche to be effectively removed from the gas in the tube. The probability of a few electrons remaining after a time lapse of a second is thus high. The mechanism of removal of electrons are those given earlier. Immediately after the avalanche recombination is most important. When most of the electrons have been removed the other two mechanisms become important.

This phenomenon is useful in cosmic ray studies for two reasons: (a) The information given by an array of tubes after traversal by a selected

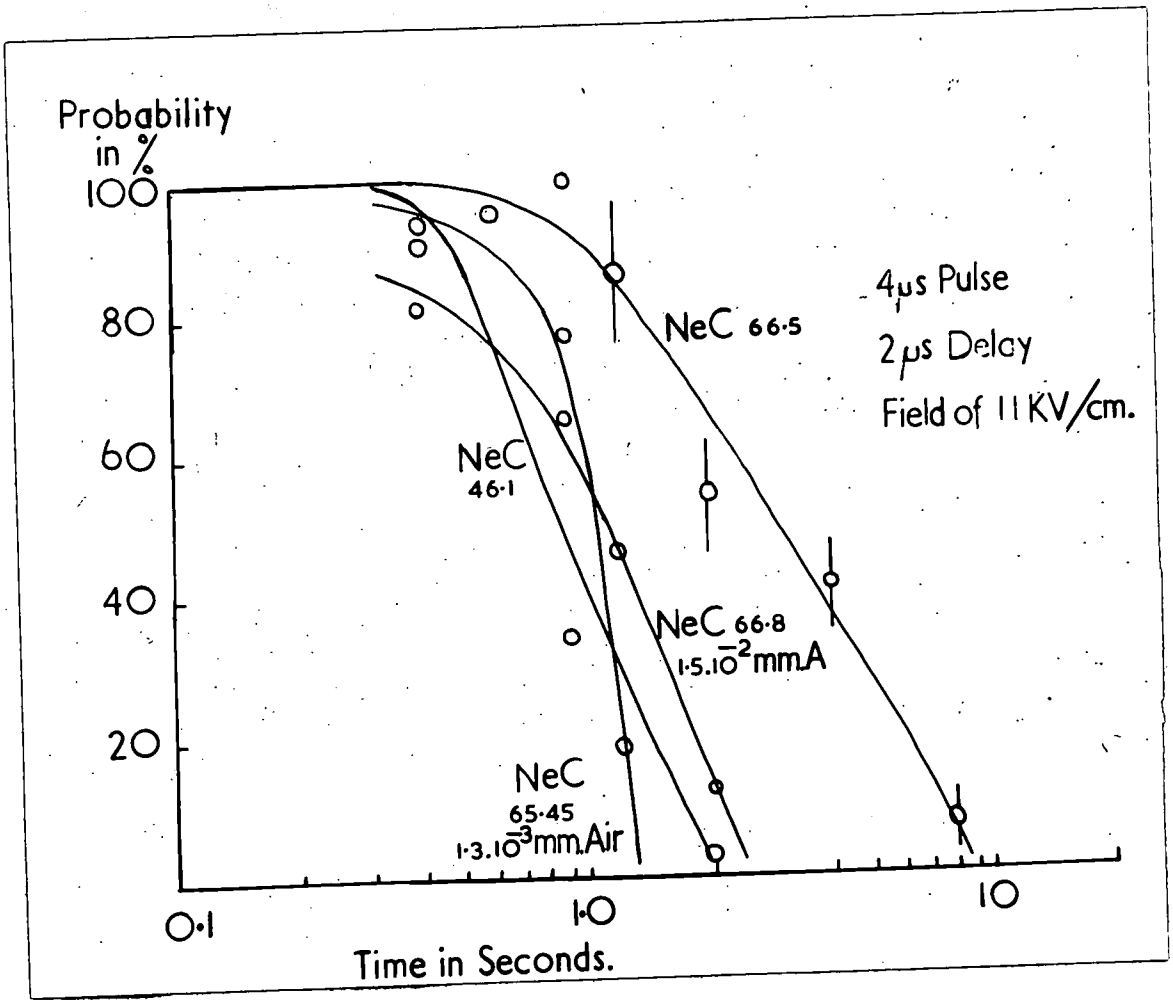

Fig. 15

Probability of After-flashing as a Function of the Time Interval between the two Pulses.

particle can be retained by repeated flashing so that, for example, a camera shutter may be opened after the passage of the particle, and (b) under certain conditions the individual flashes are weak - the photographic image can then be enhanced by repeated flashing.

V. 11. General Remarks and Conclusions

The work described in these chapters was undertaken to find a suitable flash tube which would work with high efficiencies at long delays and could be mass-produced. As a result our investigations were confined mostly to tubes filled with commercial neon and operated at time delays greater than 2 μsec. The characteristics of tubes filled with spectroscopic neon were determined at one pressure only : 35 cm Hg.

In spite of the rather different conditions of the experiments reported here and those of Conversi and collaborators the results show agreement in a number of aspects:

(i) The maximum efficiency of tubes containing spectroscopic neon at a pressure of 35 cm Hg is consistent with that found by Conversi et al for the same time delay, after allowance has been made for the different wall thickness of the tubes.

(ii) The effect of adding argon is to produce a reduction in the threshold field strength for high efficiency of flashing. (Fig 2 and fig. 11 of Barsanti et al).

(iii) There is no difference in efficiencies for pulse lengths of 2 and 4 μsec.

An important result found by Barsanti et al was the slight decrease

in the efficiency of tubes containing spectroscopic neon at 45 cm Hg, fig. 3. It is probable that the apparent reduction was due to statistical fluctuation. In our work the efficiency was found to increase with increase of pressure up to the highest pressure used.

The increase in efficiency with pressure is due to theincreased number of electrons produced in the gas by the ionising particle. The values of the primary (P.S.I.), and the total specific ionisation (T.S.I.) for different pressures is given in Table III.

TABLE III

The primary and the total specific ionisation in the gas for different pressures.

Pressure in cm Hg	66.5	60.0	50.0	40.0	30.0	25.0	20.0
P.S.I.	10.5	9.48	7.90	6.31	4.73	3.94	3.16
T.S.I.	21.0	18.95	15.80	12.12	9.45	7.88	6.31

Using these values in equation (2) the layer efficiencies are calculated. Table IV gives the observed and calculated layer efficiencies for various pressures.

TABLE IV

Comparison of the observed and the calculated efficiency for different pressures

Pressure in cm Hg	66.5	60.0	50.0	40.0	25.0	20.0
Calculated Layer Efficiency %	61.5	57.8	51.9	45.8	27.0	20.4
Observed Layer Efficiency %	62.0	59.0	50.5	41.0	25.0	18.5

The agreement between the observed and the calculated efficiencies indicate the correctness of the assumptions. It may be noted that the value of δ used in equation (2) is $0.\overset{4}{16}$ cm. This is nearly a third of the mean path length $\bar{L}$.

Contrary to the observations of Barsanti et al it is found that commercial neon can be used in flash tubes. With the higher pressures used in our experiment the impurities in commercial neon are not important in reducing the efficiency and much longer time delays can be tolerated.

As a result of the experiments described it hasbeen found possible to produce tubes of high efficiency which can be mass-produced cheaply. For example a tube constructed of Soda glass filled with commercial neon at 65 cm Hg and a residual air pressure of 10^{-3} mm Hg has an internal efficiency of 80% for a time delay of 3.7 μ-sec.

CHAPTER VI

THE DEVELOPMENT OF A PROTOTYPE SPECTROGRAPH

VI. 1. The Experimental Arrangement

Before the particle detector described in the previous chapters could be usefully applied to the location of the trajectory in the large magnetic spectrograph it was considered desirable to construct a prototype spectrograph and to study in detail its characteristics.

The schematic diagram of the prototype spectrograph is shown in fig. 16. It was first operated at sea level without the magnet with the object of studying such aspects as the accuracy of particle location and later with the magnetic field to measure the underground momentum spectrum.

Four tube arrays and associated Geiger counters served to trace the trajectories of the high energy particles at sea level. The array consisted of five layers of 15 cm tubes rigidly mounted 8.0 mm apart between parallel electrodes. The tubes were staggered at an angle such that no particle entering within the angular acceptance of the instrument ($\pm$ 10°) could pass through the dead space. The scattering was reduced by replacing the central regions of the electrodes with aluminium foil. Since the object of the experiment was to determine the limit to the spatial accuracy of location of the particle trajectories it was necessary to accept only fast particles ($p > 800$ M.e.V/$_c$) for which displacement in the apparatus by scattering was small. Thus a low momentum cut off was imposed by demanding further penetration of 55 cm of lead.

The tubes used in this experiment were filled with commercial neon

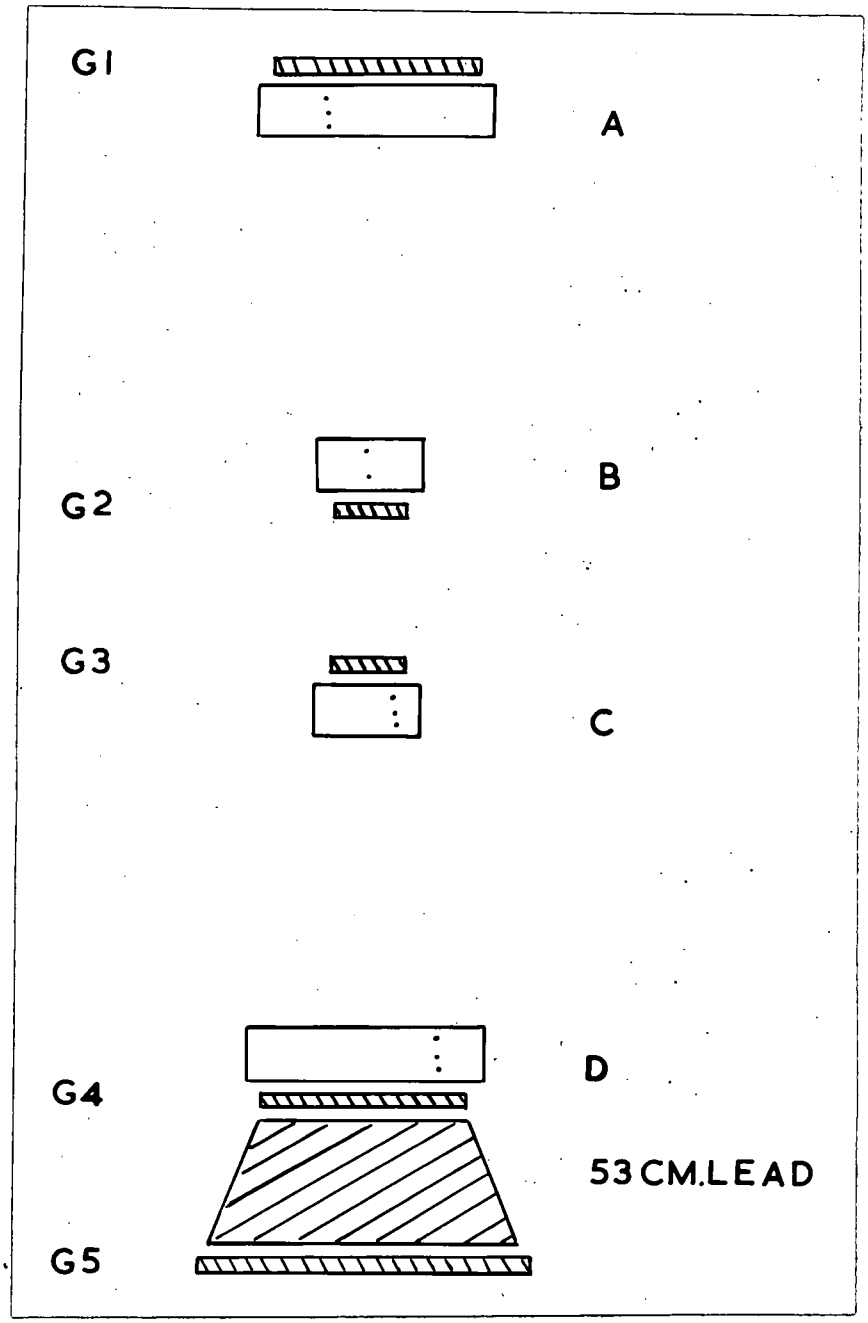

Fig. 16.

Schematic Diagram of the Prototype Spectrograph.

at 65 cm Hg and the residual air pressure was estimated to be 10^{-5} mm Hg. The characteristics of the high voltage pulse applied to the plates after a five-fold coincidence were as follows: peak height 6.5 kv/cm, time delay 2.0 μsec, rise time 0.5 μsec and pulse length 4 μsec. Under these conditions the internal efficiency of the tubes was 70% and the layer efficiency 52%.

The accuracy of location was determined from measurements made by Ashton (1958) of the angle θ between the apparent trajectories in A B and C D for a large number of particles. The distribution of this angle after correction for scattering gave the noise level or 'no field' limit of measurement. Measurements of the track directions were made by three methods:

(i) The centre of gravity of the array formed by the centres of the tubes which flashed at each level was calculated and the inclination of the line joining the appropriate pairs was determined.

(ii) A full-scale diagram of the tube assembly was drawn and cotton fibre adjusted over its surface to give the best estimate of the track location.

(iii) The photographic records were projected on to a rotatable screen ruled with close parallel lines and the directions of the line determined which satisfied the condition that the sum of the distances from the centres of the flash tube images to the line was a minimum.

In each method when a tube was observed to flash in such a position as to be incompatible with the trajectory defined by other tubes this flash was rejected. Some comments can be made on these methods. Method (i) has the advantage of being completely objective, but some information present in the record is not used. For example, the uncertainty in determining the centre of gravity of the tubes that flashed in the array A is reduced if the approximate direction of the trajectory is known from information obtained from the tubes that flashed in the array B and vice versa. Method (ii) is subjective but has the advantages that not only the excited tubes but also the gaps between the sensitive regions can be used to locate the trajectories. Method (iii) on the other hand relies on the excited tubes since these are the only images visible on the film. A basic assumption is that the image accurately represents the end of the tube, and with carefully constructed tubes this condition is satisfied.

All the photographs taken in this experiment were measured using methods (ii) and (iii) and a smaller number with method (i). It was found that method (i) gave poor results and that there was little difference between the results of (ii) and (iii). Method (iii) is quicker to apply and is indicated for application where a high particle rate is encountered. On the other hand, method (ii) gives useful additional information in that the displacement of the trajectories at the centre of the field region can be found, and this enables an independent check on the accuracy of location to be made.

The r.m.s. of θ found from the measurements with the present apparatus

is $0.35^{\circ} \pm .02^{\circ}$. This value contains components arising from (a) the scattering of particles in arrays B and C (b) the error of setting the measuring device (cross wire etc) on the best estimate of the trajectory (c) the error of interpretation, i.e. the difference between the estimated and the true trajectories, and (d) the traversal of the apparatus by more than one particle. Of these causes (c) and (d) need further amplification. Here (c) refers to cases where one or more of the tubes discharged were not traversed by the ionising particle itself. Probably the most important contribution arises from unrecognised knock-on electrons e.g. a case when a fast particle passes through the insensitive region of one tube and an associated knock-on electron passes through the next tube such that a systematic difference between the best estimate and the true trajectory cannot be recognised.

The contribution from scattering and errors of setting are known and thus the error from the combination of (c) and (d) can be determined. Writing σ_{sc}, σ_{s}, σ_{rem} for the root - mean - square deflections due to the scattering setting and the remaining causes we have $\sigma_{sc} = 0.22^{\circ}$, $\sigma_{s} = 0.14^{\circ}$, giving $\sigma_{rem} = 0.20 \pm .03^{\circ}$. It is usual to quote the uncertainty as that of position at a single level (e.g. the middle of each array) and this can be calculated, but it must be borne in mind that this uncertainty is less than would be found if the single level alone were observed on account of the information on direction given by the combined data from the two levels.

The required r.m.s. error is given by

$$\delta = \frac{L \cdot \sigma_{rem}}{2}$$

Where L is the separation of each pair of the measuring levels. The result is

$$\delta = (0.62 \pm .10) \text{ mm.}$$

VI. 2. Conclusions

A comparison can be made between this method and the cloud chamber. In a cloud chamber at normal pressures the inherent track width for cosmic ray particles is ~ 1 mm, being determined by the diffusion of the ions before their fixation by the condensation of the condensant. It is possible to determine the centre of the track to within about 0.2 mm, but to this uncertainty must be added that arising from gaseous distortion. By careful temperature control distortion can be reduced, but both short and long term variations in distortion produces difficulties. In the Manchester high-energy spectrograph (Holmes et al 1955) cloud chambers were used as detectors and the overall uncertainty in track location was shown in a subsidiary experiment by Lloyd et al (1957) to be about 0.8 mm. Further reduction by more careful temperature control is presumably possible but the location uncertainty in a cloud chamber is inherently variable and in that respect alone is inferior to the flash tube array with its constant geometrical uncertainty. It is apparent that a further reduction in the error of location can be made in the flash tube array by increasing the number of layers, an upper limit being set by the maximum tolerable

scattering uncertainty. Some further increase is also possible by the use of tubes having higher internal efficiency and efforts were made in this direction before constructing great numbers of tubes required for the Durham spectrograph.

CHAPTER VII

THE CHARACTERISTICS OF HIGH PRESSURE TUBES

VII. 1. The Description of the Apparatus

The fact that the experimental curve, fig. 10, of the variation of efficiency with pressure of neon showed a steady increase up to 65 cm Hg encouraged the investigation of tubes filled at pressures higher than one atmosphere. Since it was found in the experiments described in Chapter 5 that air pressures up to 10^{-4} mm Hg gaveno appreciable reduction in the maximum efficiency of the tubes, the process of baking the tubes was dispensed with. The filling system was modified (fig 17) so that tubes could be immersed in liquid nitrogen prior to sealing off. A trolley capable of movement along the length of the manifold carries the Dewar flask containing liquid nitrogen. The Dewar flask is raised by a pulley system so that suitable lengths of the tube could be immersed.

The pressure of the neon in the tubes is evaluated in the following manner. If lo is the length of the tube (from the flattened end to the constriction) and if l_1 is the length immersed in liquid nitrogen, then the following relation holds between the pressures of the gas before and after sealing.

$$\frac{p_i\, l_1}{(273-195.8)} + \frac{(lo - l_1)\, p_i}{273 + 20} = \frac{p_f\, lo}{273 + 20}$$

where p_i is the pressure of gas in the tube while itis immersed in liquid nitrogen and p_f is the final pressure when the tubes attain room temperature. The temperaturesof liquid nitrogen and the room are -195.8° c

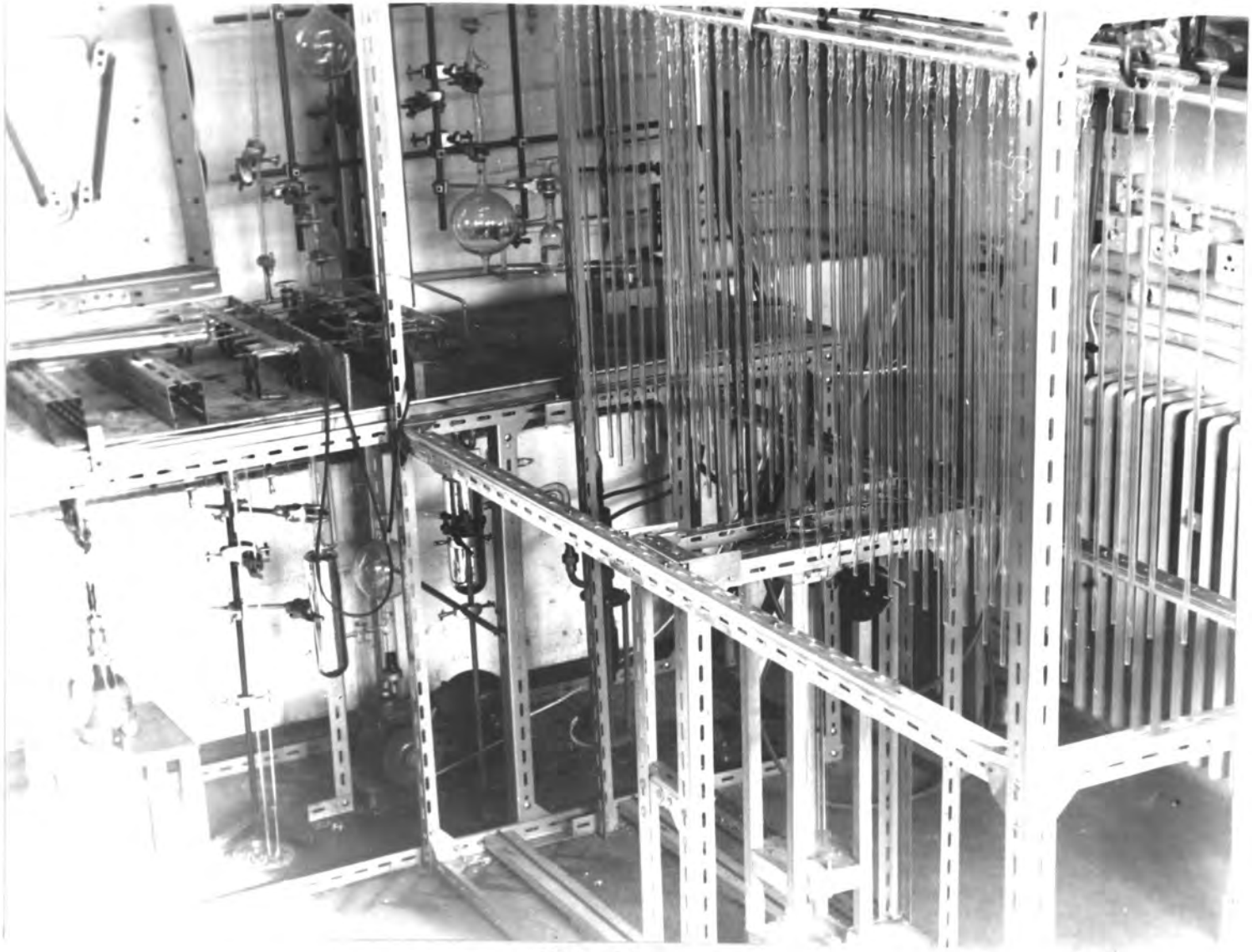

Fig. 17.

Photograph of the Modified Filling System.

and 20° c respectively. It will be seen that with almost total immersion ($l_i = l_o$) the pressure attainable is 3.8 π where π is the atmospheric pressure. At a later stage a check was made on the values of the pressure evaluated in this manner by determining the pressure of the neon in the tubes experimentally. It was found that the calculated values were within 5% of the experimental value. Three batches of tubes were filled at pressures of 3, 2.2 and 1.3 atmospheres. A further batch of tubes at 0.8 atmospheres was included when the efficiencies were measured.

Since the area of the stacks carrying the flash tubes in the big spectrograph was to be 7000 cm^2, the electrostatic capacity of eight layers would be of $\sim 2 - 3$ thousand p.f.s. This comparatively large capacity would cause a considerable increase in the rise time of the high voltage pulse and consequently reduce the efficiency of the tubes. To obviate this difficulty it was decided to pulse the stacks from separate generators. This demanded the use of a large number of hydrogen thyratrons (XH8). The prohibitive cost of the latter favoured their replacement by trigatrons (CV 85). The circuit employed is shown in fig. 18. A 0.5 μsec delay line discharging through the hydrogen thyratron produces the necessary trigger pulse of 3 kV for the trigatrons. Several trigatrons were operated from the same trigger pulse. The 100 K resistor served to prevent the quenching of the trigger voltage across the trigger gaps.

VII. 2. The Variation of Efficiency with Field Strength

The efficiencies of the high pressure tubes were measured for field strengths ranging from 3 kv/cm tp 7 kv/cm. The assembly of tubes and the

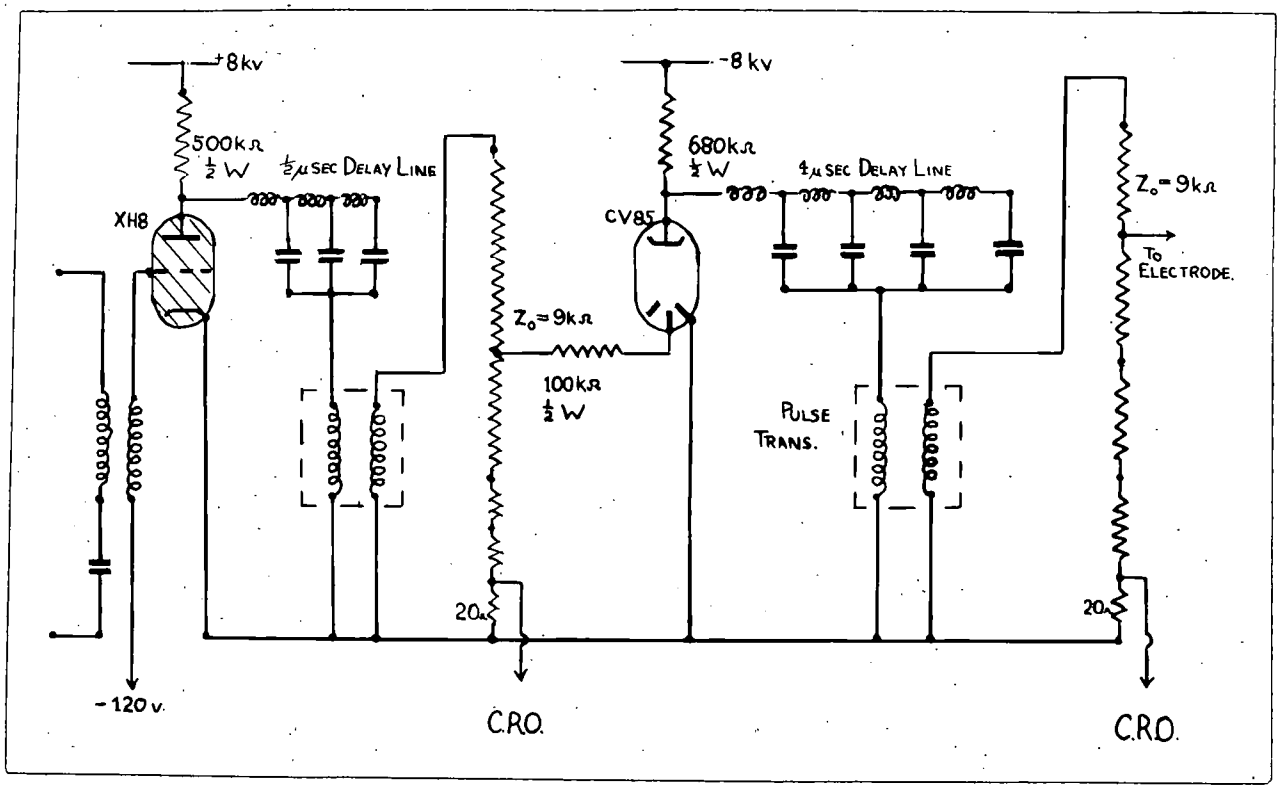

Fig 18.

The Modified Pulse Generator.

experimental arrangement were similar to the one described earlier. Efficiencies at field strengths higher than 7 kv/cm were not measured as the constancy in the plateau region is well-known.

Fig. 19 shows the variation of the layer efficiency with field strength. The maximum layer efficiency of the tubes containing neon at a pressure of 65 cm Hg and 10^{-3} mm Hg air was 40% for a pulse having τ = 3.5 μ-sec. This is rather lower than the values found earlier but is not statistically inconsistent. It is interesting to note that the maximum efficiency of tubes containing neon at 1.3 π cm Hg is 57% whereas the corresponding values for tubes containing neon at 2.2 π and 3.0 π cm Hg are as high as 70%. These results clearly demonstrate the expected trend of increasing efficiency with pressure.

Another important feature of the curves is that the efficiency for the different tubes reaches 90% of the maximum value at the same field strength of ~5 kv/cm indicating that the significant quantity is not E/p but simply E. The significance of this is discussed in the next chapter.

Some photographs of the flashes obtained by Mr. H. Coxell and the author are shown in Plate 1.

VII. 3. The Variation of Efficiency with Time Delay

The maximum efficiencies of the tubes at time delays varying from 4 to 24 μ-sec were measured. Here again the range of the delay times chosen was dictated by the values expected in the spectrograph. The results are shown in fig. 20. They indicate that high pressure tubes have a slower

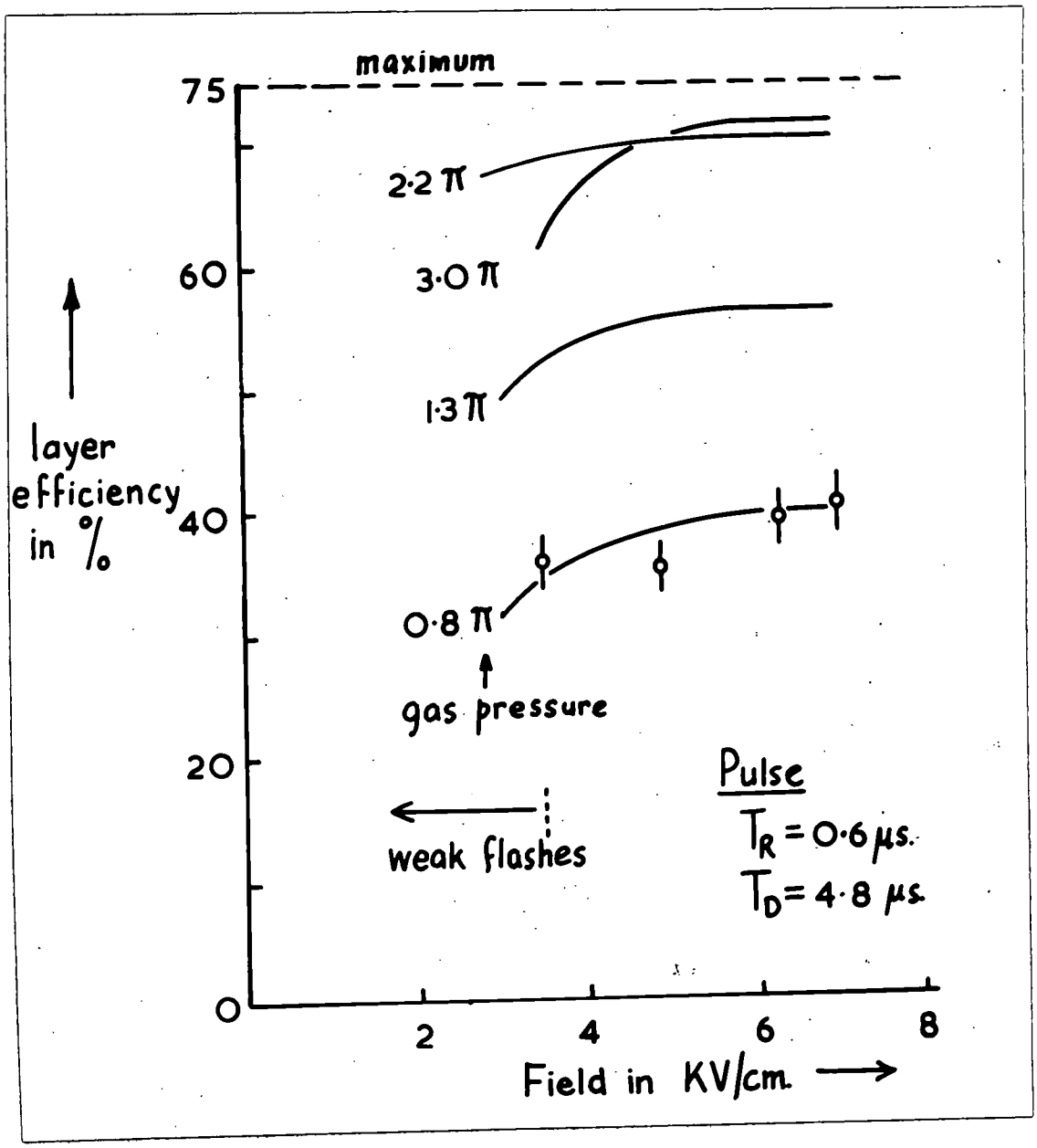

Fig. 19.

The Variation of Efficiency with Field for Different Pressures of Neon

Single Ionising Particle

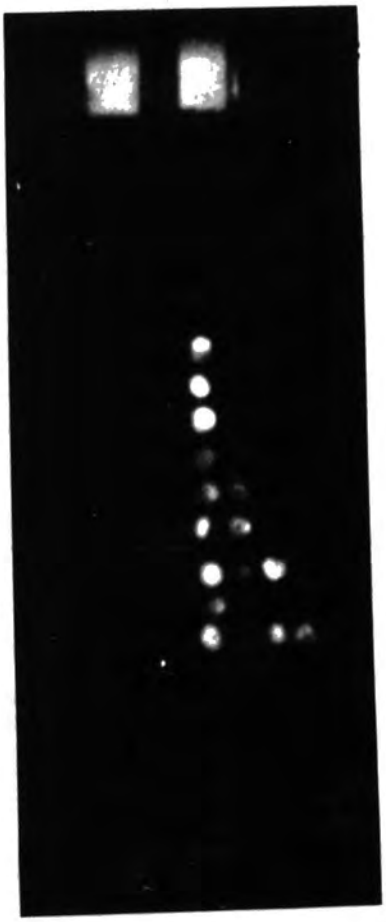

Knock-on Electrons produced in the Tube Assembly

Plate 1

Photographs of the Flashes

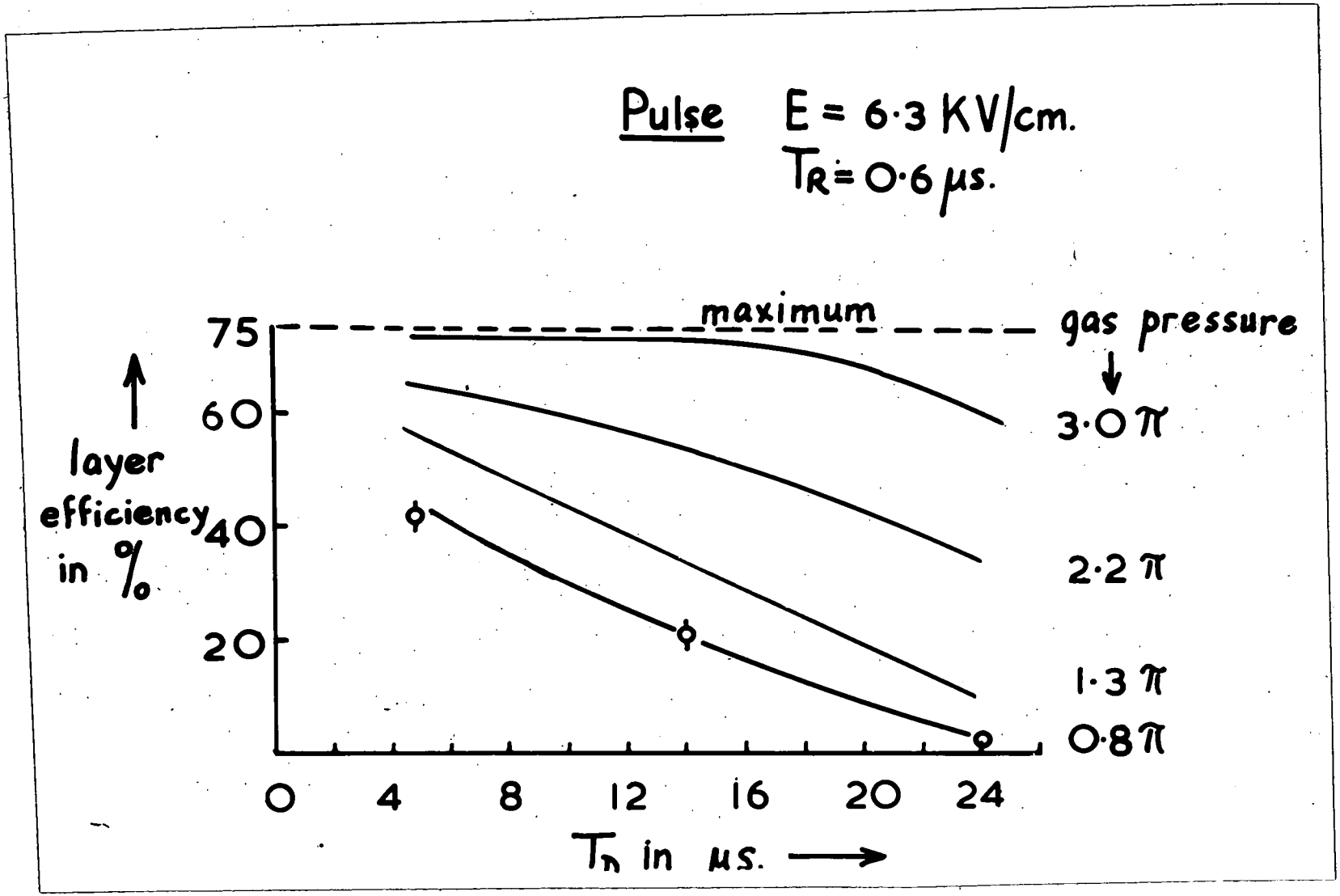

Fig. 20.

Variations of Efficiency with Time Delay T_D

rate of fall of efficiency with time delay. The 3 π tubes have an efficiency of ~60% at time delays of 24 μsec compared with 3% for tubes containing neon at 65 cm Hg.

VII. 4. The Variation of Efficiency with the Wall-thickness of the Tubes

The advantages of using thin walled tubes in the spectrograph are that it reduces the total dead space in each array and the occurrence of flashes from knock on electrons.

Efficiency measurements were made on compound tubes consisting of three sections each having nearly the same internal diameter but different wall thicknesses (0.4 mm, 0.9 mm and 1.2 mm). Each 'tube' contained the same gas at 1.5 π cm Hg. Fig. 21 shows the variation of absolute effidency for the three thicknesses.

The 30% difference in absolute efficiencies between the medium and thin tubes is most unexpected. This result seems to indicate that the glass thickness plays an important role in the discharge mechanism. A possible mechanism that could account for this difference is discussed in VIII. 4.

VII. 5. The Effect of the Clearing Field on the Efficiency of the Tubes.

It is apparent from fig. 20 that at high pressure the efficiency falls off slowly with increasing time delay. Thus the sensitive time of the high pressure tube, defined as $T_s = \int_{-\tau}^{\infty} \eta\,(t)\,dt$ is very long. For example at a pressure of 2.5 atmospheres T_s = 39 μ-sec. Thus if the particle rate is high an appreciable fraction of accidental flashes will result. Efforts

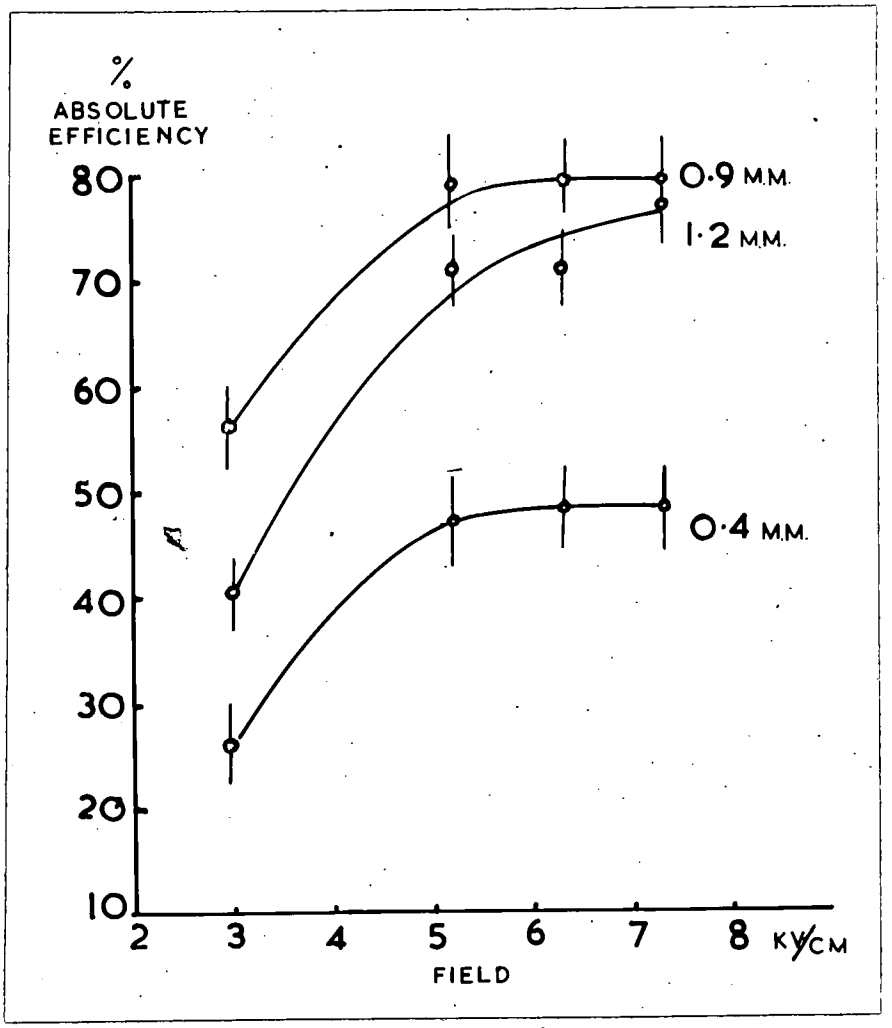

Fig. 21

The variation of Absolute Efficiency with Field for Different Wall-thicknesses of the Tubes.

were therefore made to reduce T_s by applying a clearing field across the electrodes. This procedure is analogous with that in the cloud chamber where the clearing field sweeps out unwanted ions arising from pre-expansion particles.

The efficiency of the tubes was measured for various time delays when a steady potential was maintained between the plates of the tube assembly. The clearing field used varied from 70 volt/cm to 2 kv/cm. The experiment was also repeated with the polarity of the steady field reversed. The effect of the clearing field on the efficiency was barely noticable even for large values of T_D viz 20 - 30 μ-sec.

It can be shown that for a field strength of 2 kv/cm the transit time of an electron across the tube is less than 0.5 μ sec and a considerable reduction in T_s should result. It is difficult to explain the results on the present gas discharge mechanism. The significance of this result is discussed in some detail in Chapter VIII.

VII. 6. Lifetime of Tubes.

Flash tubes containing a pure inert gas such as neon might be expected to have an almost infinite life-time. However, impurities present in the gas filling and others introduced from the glass wall by the impact of ions could reduce its life-time. An experiment was therefore carried out in which a set of tubesof previously measured efficiency was subjected to pulses at the rate of 1 per second for 13 days. A 10 millicurie γ -ray source (Ra-Be) produced flashes in the tubes for about 70% of the pulses. The total number of flashes was about 10^6 for each tube. The efficiencies

were measured again at the end of the experiment. The characteristics of the pulse were E_{max} = 10 kv/cm T_R = 0.6 μsec, τ = 3.5 μsec.

TABLE V.

The variation of efficiency with the 'life' of the tube

Time delay T_D in μsec.	4	40
Percentage Efficiency at start.	97.5 ± 3.7	47.0 ± 2.8
Percentage Efficiency after 10^6 pulses	94.5 ± 3.4	35.5 ± 2.9

Table V shows that there is no significant difference in the efficiency for short delay times but at 40 μsec there is a reduction of about 12%. This reduction is perhaps due to the appearance of small amounts of occluded gases from the wall of the tube or a change in the structure of the glass under continuous bombardment by neutrons and γ- rays. This change in characteristics is, however, unlikely to be important in practice.

VII. 7. Discussion and Conclusion.

To facilitate the choice of optimum pressure an investigation has been made of the possibility of establishing a universal relation between the efficiency and some function of time delay and pressure. The single parameter T_D/p was found to be applicable and fig. 22 shows the variation of (absolute efficiency) with T_D/p In addition to the efficiency measurements

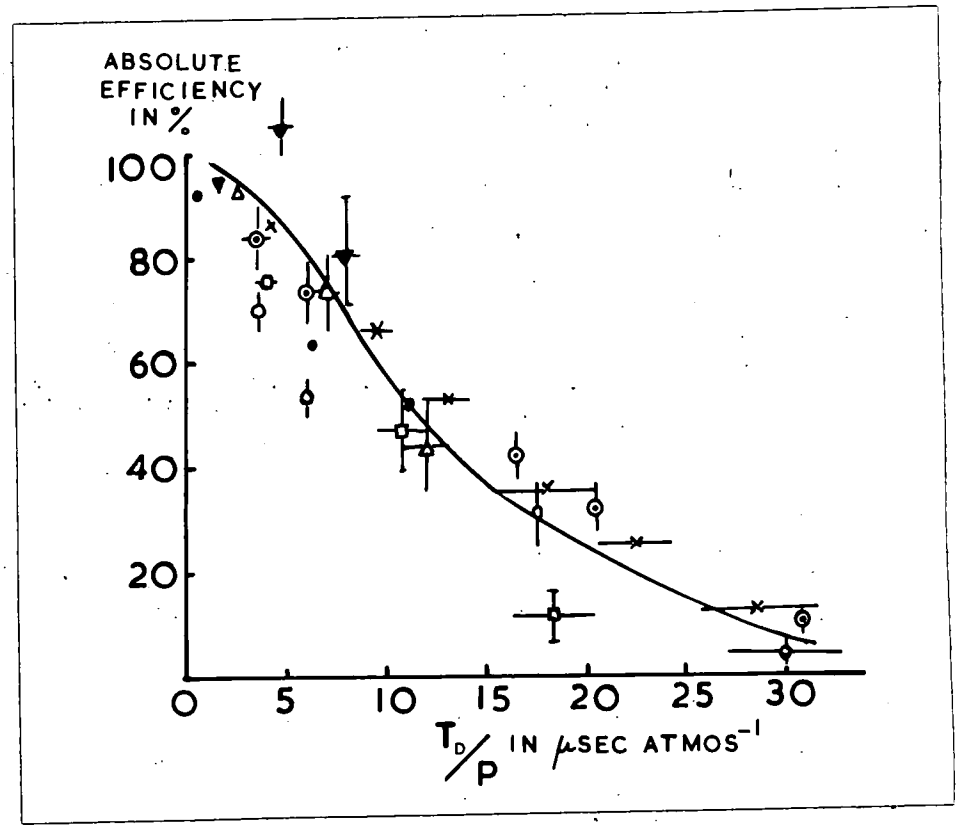

Fig. 22.

The Variation of Efficiency with the Ratio of Time Delay to Pressure.

Pressure in Atmospheres	0.26	0.6	0.8	1.3	2.0	2.5	3.0
Experimental Points	•	⊙	○	□	△	×	▼

made in the present work those of Conversi et al for a pressure of 20 cm Hg have also been included. The results shown in fig. 22 therefore refer to a pressure range of a factor of 10 and it is apparent that the simple relation $\eta = \left(\frac{T_D}{p}\right)$ where f is an unknown function holds to a fair approximation over this range. The efficiency for a given time delay can now be determined to a fair accuracy for pressures between 20 cm Hg and 5 atmospheres and to a lesser accuracy for pressures outside this range.

The significance of the fact that T_D/p appears to be the operative parameter, when the remaining parameters E_{max}, T_R and τ are kept constant may be seen from a consideration of the simple theory discussed in Chapter V.7 (b). There it was shown that for short time delays $\eta(T_D)$ is given by

$$\eta(T_D) = \eta(o)\left\{1 - \exp -N_b\left(1 - \frac{\delta}{L}\right) f\left(\frac{R^2}{4D\,T_D}\right)\right\}$$

The diffusion coefficient D is proportional to $\frac{1}{p}$ and therefore $\frac{T_D}{p} \propto D\,T_D$ and since we have found $\eta(T_D)$ is a function only of $\frac{T_D}{p}$ at constant R, this must be interpreted as indicating that $n\left(1 - \frac{\delta}{L}\right)$ does not depend on the gas pressure. However, n is proportioned to p and so the length of the track effective in producing an avalanche must fall with decreasing pressure. This fact together with the other difficulties mentioned earlier indicates that the mechanism of the discharge at high pressures ($\gtrsim 0.8$ atmosphere) is probably different from that at low pressure.

In the next chapter the various mechanisms of spark discharge are described and their relevance to the present measurements considered.

CHAPTER VIII

THEORETICAL ASPECTS OF THE MECHANISM OF THE FLASH TUBE

VIII. 1. Basic Discharge Mechanisms.

A detailed study of the variation of the current between parallel plane electrodes in a gas as a function of the applied voltage wasmade by Townsend (1939). He introduced the fundamental coefficient α to define the number of electrons produced per centimetre in the path of a single electron travelling in the direction of the field. The electrons so formed gain energy from the field and produce additional electrons by collision. The resulting current in the space betweenthe electrodes is given by

$$i = \ell_0 e^{\alpha d} \quad \ldots\ldots\ldots\ldots (6)$$

where d is the distance between the electrodes and ℓ_0 the current produced by the external source of light falling on the cathode. Equation (6) was found to be valid for limited values of the field strength. When the field strength was increased beyond a certain limit the current increased at a more rapid rate indicating that secondary mechanisms occur. The secondary ionisation in the gap has been attributed to various causes. The most probable of these is the secondary emission of electrons from the cathode by the impact of the positive ions and photons. If γ is the number of electrons released from the cathode per indident positive ion then the resulting current is

$$i = \frac{i_0 \, e^{\alpha d}}{1 - \gamma (e^{\alpha d} - 1)} \qquad (7)$$

A similar equation has been derived by Loeb (1939) for the case where

secondary emission from the cathode is caused by photon impact. The current is then

$$i = \frac{i_0 \, e^{\alpha d}}{\alpha - \theta \varepsilon g \left[e^{(\alpha-\mu)d} - 1 \right]} \qquad \ldots\ldots\ldots\ldots (8)$$

where θ is the number of photons produced by an electron per cm in the field direction, g is the geometrical factor giving the fraction of photons created in the gas that reach the cathode, μ is the absorption coefficient of the photons in the gas and ε the fraction of the photons which produce electrons that succeed in leaving the cathode. Equation (8) can be shown to be very similar to equation (7). Thus we may represent the current by equation (6) where γ may represent one or more of the several secondary mechanisms.

The value of $(e^{\alpha d} - 1)$ is zero at low field strengths but increases as the field strength is increased until we have

$$\gamma \left(e^{\alpha d} - 1 \right) \qquad \ldots\ldots\ldots\ldots\ldots (9)$$

when the denominator of equation (7) becomes zero and the equation becomes indeterminate. This condition according to Townsend defines the sparking threshold. It has been observed in all casesof breakdown that $\gamma e^{\alpha d} \gg 1$ and thus the Townsend criterion reduces to

$$\gamma e^{\alpha d} = 1$$

It has been shown by Loeb (1948) that if $\gamma e^{\alpha d} < 1$ the discharge is given by equation (7) but the current is not self maintained, i.e. the current reduces to zero if the external source of radiation is removed. For $\gamma e^{\alpha d} = 1$ the number of additional ion pairs produced in the gap by the passage

of one electron is large enough for the resultant positive ions to release another from the cathode and thus to cause a repetition of the process. The discharge is then self sustaining and can continue in the absence of the source. Thus $\gamma e^{\alpha d} = 1$ defines the sparking threshold. If $\gamma e^{\alpha d} > 1$ the discharge grows more rapidly due to the cumulative effect by successive avalanches.

The Townsend criterion $\gamma e^{\alpha d} = 1$ has been found to be in agreement with experiments for breakdown of gases at low pressures. On the basis of secondary electron production by positive ion bombardment one expects a formative time due to the low mobility of the positive ions. Much higher speeds of formation have been observed in studies of long sparks at atmospheric pressure and in the breakdown of gaps subjected to impulse voltages. Further, in the study of spark discharge between a positive point and a negative plane, the impulse breakdown voltage appears to be independent of the cathode material.

Various modifications to the Townsend theory have been put forward by different workers. A theory of the spark applicable especially to sparks occurring between gaps at atmospheric pressure and above was proposed by Meek (1940) and independently by Raether (1940). This theory has been elaborated by Loeb (1941), Meek, (1941) and others and is generally referred to as the streamer theory of the spark. This theory involves the assumption that the ionisation processes is dependent only on the gas. An electron from the cathode in moving a distance x in the direction of the field creates an additional $e^{\alpha x}$ ions. In short gaps of ~1 cm the first electron avalanche

leaves behind a dense cloud of positive ions near the anode. For values of $\alpha = 17$ there are about $1.2.10^7$ ions near the anode. Such a distribution of ions does not constitute a breakdown of the gap. If we assume the positive ions to be concentrated in a sphere of radius $\bar{r}$ the field strength due to this space charge at the surface of the sphere is $q \in /\bar{r}^2$ where q is the number of charges in the sphere and ϵ is the electronic charge. The number of charges is equal to $\frac{4}{3} \pi \bar{r}^3 N$ where N is the density. Thus the field produced by the space charge is

$$E_r = \frac{4}{3} \pi \bar{r} \; N \epsilon$$

The density of ions, N, can be shown to the equal to $\alpha e^{\alpha x} / \pi \bar{r}^2$ and the expression for E_r becomes

$$E_r = \frac{4}{3} \frac{\epsilon e^{\alpha x}}{\bar{r}} \quad \ldots\ldots\ldots\ldots\ldots\ldots (10)$$

Now $\bar{r}$ is the value caused by electron diffusion in crossing the gap and is given by $\bar{r} = \sqrt{2Dt}$ where D is the diffusion coefficient and $t = \frac{x}{kE}$

where k is the electron mobility and E the applied field strength. Thus equation (10) reduces to

$$E_r = \frac{4/3 \, \epsilon \alpha \, e^{\alpha x}}{\sqrt{\frac{2D}{k} \cdot \frac{x}{E}}}$$

From a consideration of the ratio $\frac{D}{k}$ for electrons Loeb (1941) and Meek (1941) show that E_r can be written in the form

$$E_r = \frac{4/3 \; \epsilon \alpha \; e^{\alpha x}}{\left(1010 \; \frac{2x}{5p} \; \frac{\lambda_o}{\sqrt{f}}\right)^{\frac{1}{2}}} \quad \ldots\ldots\ldots\ldots (11)$$

Where λ_o is the electron mean free path at 760 mm Hg, f is the average fraction of energy lost per impact and p is the pressure in mm Hg. Equation (11) in the case of air becomes

$$E_r = 5.7 \times 10^{-7} \frac{\alpha e^{\alpha x}}{\left(\frac{x}{p}\right)^{1/2}} \quad \text{volts/cm}$$

This field augments the externally applied field E, the magnitude of the the total field becoming $\vec{E}_r + \vec{E}$.

Accompanying the cumulative ionisation of the first avalanche is a larger number of excited atoms and molecules. The excited atoms emit radiation which is absorbed by the gas. The photo-electrons produced in this process if they happen to be suitably situated near the space charge are accelerated towards it and produce smaller avalanches which feed into the positive space charge. In this way a positive space charge develops towards the cathode as a self-propagating streamer. The velocity of these streamers have been observed to be $\sim 2.10^7$ cm/sec. When the streamer reaches the cathode the space between the electrodes is rendered highly conducting and a spark ensues.

The conditions necessary for a streamer to develop depend on the pressure of the gas and the absorption coefficient of the photons in the gas. If the first avalanche is diffuse and broad, and the absorption of the photo-electrically active radiations small, streamer formation is unlikely. According to Loeb (1941) the condition for sparking in a parallel-plane gap is obtained from equation (11) by setting $E_r = E = E_s$ where E_s is the sparking threshold. For air the sparking threshold can be obtained from equation (12)

$$\alpha d + \log_e \frac{\alpha}{p} = 14.46 + \log_e \frac{E_s}{p} + \frac{1}{2} \log_e \frac{d}{p} \quad \ldots (12)$$

where d is the separation between the plates and p the pressure of the air.

Since the theory for the breakdown of the gaps when small particles of insulating materials, such as porcelain and rutile, are present on the electrode surfaces is different from those outlined above, a brief summary of the mechanism supposed to be responsible for their breakdown is given. The study of Slepian and Berkey (1943) showed that the time lag of the gap is reduced by the presence of particles of average linear dimensions between 0.002 and .015 cm. It is considered that these particles cause localised intense field distortions at the electrode surfaces so that the rate of electron emmission from the cathode is increased. It is also reported that in some experiments a pre-breakdown corona is followed by the spark. It has been suggested that the radiation emitted from minute corona discharges at the projections could cause photoionisation in the gas and bring about the ultimate breakdown of the gap.

VIII. 2. Application of the Spark Theory to Flash Tubes.

(a) Low Pressure Tubes.

The curves of figures 2 and 8 show that the efficiencies of the low pressure tubes attain 90% of their maximum value at a field strength of ~5 kv/cm . This we shall term the sparking threshold. If a spark is to

occur under these conditions, the Townsend criterion $\gamma e^{\alpha d} \geq 1$ must be satisfied. In evaluating the value of γ necessary to satisfy this criterion we shall assume the values of α for pure neon as there are no published results on commercial neon. This is justified as we are only concerned with the orders of magnitudes of the quantities involved. For tubes at 65 cm Hg, E/p = 7.6 volts/mm and $\frac{\alpha}{p}$ = .0204 giving αd = 7.9 where d is the diameter of the tube. The Townsend criterion gives

$$\gamma e^{7.9} = \gamma\, 2.7 \times 10^{3} \geq 1$$

Thus the value of γ must be $\geq 3.10^{-4}$. In the case of impulse breakdown the contribution to γ comes only from the impact of photons on the cathode. From Geiger counter studies it is known that about 100 to 1000 photons liberate 1 electron from the cathode. If we assume a similar value for glass the discharge in the low pressure tubes can occur according to the Townsend mechanism.

(b) <u>High Pressure Tubes</u>.

Fig. 19 shows the sparking threshold to be also about 5 kV/cm in the pressure range (0.8 - 3.0) π. Corresponding to the value of $\frac{E}{p}$ = 2.2 volts/cm/mm αd has a value 1.08. If the Townsend criterion is to be satisfied in this case γ has to assume values $\geq$ 0.5, a value 50 times that observed for metal cathodes like copper. Thus it is unlikely that Townsend's mecahnism can operate in the high pressure neon tubes.

With the help of equation (12) we can calculate the sparking threshold for the high pressure tubes. Equation (12) for neon is given by

$$\alpha d + \log_e \frac{\alpha}{p} = 13.7 + \log_e \frac{E_s}{p} + \frac{1}{2} \log_e \frac{d}{p}$$

The value of E_s which makes the L.H.S. of the above equation approximately equal to the R.H.S. is found to be ~ 13.1 kv/cm. Thus the approximate sparking threshold for 3 π tubes is 13 kv/cm. However, sparks can occur at 5 kv/cm if there is a source of electrons other than those produced in the gas.

VIII. 3. A Possible Mechanism for the Operation of High Pressure Tubes.

In the search for a source of electrons to sustain the discharge on is led to examine the portion of the glass tube in which the incident particle creates ion pairs. A fast μmeson produces about 3,000 ion pairs in the wall (0.9 mm) of the glass tube. The electrons in the medium, under the action of the electric field can move towards the surface of the glass tube and build up a surface charge. The existence of such a phenomenon has been observed in the study of semi-conductors bombarded by nucleons and electrons. Using electronsof energy ~ 1 M.e.V to bombard semi-conductors such as germanium crystals Rittner (1948) and others have observed conductivity pulses which decay with time. These pulses have been observed to last for ~ 10 μsec. They have also observed a decrease in the resistance of the crystal by a factor of 10. In the case of glass this effect may not be so pronounced due to the peculiar structure of glass.

We shall assume that such a surface charge can be produced in the glass

and then shall treat the case where the incident particle passes along the diameter (d) of the tube. If N_{gl} is the number of electrons produced in the glass at the instant the ionising particle passes through, the number left in the glass after a time delay T_D can be expected to be given by

$$N_{gl}\, e^{-\frac{T_D}{\tau_0}} \qquad \ldots\ldots\ldots\ldots\ldots\ldots \quad (13)$$

where τ_0 may be termed the 'relaxation' time. When a step pulse E volts/cm is applied the electrons drift towards the inner surface of the tube and build up a surface charge. If the combined electric field due to the surface charge and the external field is sufficiently high $(> V_0)$ field emission of electrons takes place. As the electrons come out of the surface the surface charge decreases and when a certain number has succeeded in entering the gas the emission ceases. The number emitted can be assumed to be a function of the electric field E, the number of electrons available in the glass, and the duration of the pulse (τ). Those electrons coming out first will be accelerated in the region of the intense localised field and can produce further electrons by ionisation. Thus to a first approximation we can take the number of electrons near the region of the localised field to be given by

$$F\left(N_{gl}\, e^{-\frac{T_D}{\tau_0}}, E, \tau\right) e^{\int_0^{\Delta x'} \alpha' \, dx}$$

where F is an unknown function, α' is the value of the Townsend coefficient in the region of the localised field and $\Delta x'$ the extent of the localised field.

Each of these electrons is now drawn towards the anode and produces further electrons in the uniform field E where the Townsend coefficient is assumed to be α. Thus the number of electrons in the first avalanche is

$$F\left(N_{ge}^{-\frac{T_D}{\tau_0}}, E, \tau\right) e^{\int_0^{\Delta x'} \alpha' dx} \cdot e^{\alpha d}$$

To this must be added a certain number contributed by the electrons produced in the gas by the ionising particle. At the lapse of time T_D the number of electrons left in the gas is given by

$$N_{gas}\left(1 - \frac{\delta}{d}\right)\left(1 - e^{-\frac{R^2}{4DT_D}}\right) f\left(\frac{R^2}{4DT_D}\right)$$

where d = 2R and D is the diffusion coefficient. (See Chapter V. 7.(b)). We can assume these to be accelerated across the same distance d as those produced in the glass. Thus the total number of electrons produced near the anode in the first avalanche is

$$N_s = \left[F\left(N_{ge}^{-\frac{T_D}{\tau_0}}, E, \tau\right) e^{\int_0^{\Delta x'} \alpha' dx} + N_{gas}\left(1 - \frac{\delta}{d}\right)\left(1 - e^{-\frac{R^2}{4DT_D}}\right) f\left(\frac{R^2}{4DT_D}\right)\right]^{\alpha d} \quad \text{e..(14)}$$

This is also equal to the number of positive ions produced near the anode. Following Meek (1954) we can assume these positive ions to be confined within a sphere of radius $\bar{r} = \sqrt{2Dt}$ where t is the transit time of the first avalanche. Accompanying the avalanche is a large number of photons. The photo electrically active radiations produced is assumed to be a fraction of the total number N_s. Thus the number of photons radiated within the (useful) solid angle in the direction of the cathode is given by

$$f_2 N_s \frac{d\Omega}{4\pi}$$

where f_2 is a numerical constant and $d\Omega$ is the solid angle of that part of the sphere facing the cathode.

If the absorption coefficient of the photons in the gas is μ then the number of electrons produced within a distance $\bar{r}$ and $\bar{r} + \Delta x_2$ is to a first approximation given by

$$f_2 N_s \frac{d\Omega}{4\pi} \left(1 - e^{-\mu \Delta x_2}\right)$$

where Δx_2 is the region over which the space charge field extends. Each of these electrons is now accelerated towards the positive space charge and produces further electrons. If α'' is the Townsend coefficient in the combined vector field of the space charge and the external field, the number of positive ions produced near the space charge is equal to

$$N = f_2 N_s \frac{d\Omega}{4\pi} \left(1 - e^{-\mu \Delta x_2}\right) e^{\int_0^{\Delta x_2} \alpha'' dx} \quad \ldots\ldots (15)$$

The condition necessary for the streamer to propagate itself is $N \geq 1$. If N has a large value the probability of the streamer failing to cross the gap is small, and if N is less than 1 the probability islarge. Thus the probability that the streamer will not develop when N positive ions are produced is given by e^{-N} The probability of the streamer developing under the same conditions is $1 - e^{-N}$. Since a flash is only observed if streamers develop we can write the probability of a flash occurring as η where

$$\eta = \left(1 - e^{-N}\right) \quad \ldots\ldots (16)$$

where η is thus the absolute efficiency of the tube.

VIII. 4. Interpretation of the Results.

On the basis of this mechanism an attempt is made to explain the characteristics of the high pressure tubes. The most important results to be explained are the following:

(a) For the pressures investigated viz. 0.8 π to 5 π the sparking threshold is ~ 5 kv/cm and is found to be independent of the pressure of neon.

(b) For a given time delay the efficiency increases with increase of pressure.

(c) The efficiency decreases with increasing values of time delay.

(d) The efficiency depends on the pulse width and the rise time.

(e) There is no significant reduction in the efficiency with a clearing field of either polarity.

(f) The maximum efficiency for thin walled tubes is lower than the corresponding value for tubes of greater wall thickness.

These results can be understood on the model described above. The emission of electrons from the glass commences when the localised field strength attains a value $>$ Vo. The magnitude of Vo depends on the surface charge and the applied field E. Thus we can expect the threshold for emission of electrons to be independent of the pressure of the gas, though at very high pressures a small number of electrons may diffuse back to the surface of the glass.

For a given time delay T_D and field intensity E the efficiency η can increase with increase of pressure due to the rapid increase of the absorption coefficient μ. As already noted the value of α for $E/p \leqslant 2$ does not affect the expression (16) by an appreciable amount.

From equation (13) it is seen that the variation of efficiency with time delay T_D is exponential in character.

When a step pulse is applied the emission of electrons does not take place instantaneously. The time taken for the emission to cease depends on the rate at which the surface charge decreases. Thus, if the duration of the applied pulse is made less than the time taken for the emission of electrons, the efficiency will decrease. Barsanti et al observed the

efficiency to decrease for pulse widths < 2 μsec. With a slowly rising field the electrons that are emitted when the localised field is $>$ Vo will produce a smaller number of additional ions than those produced at a later instant when the applied field has risen to a higher value. Thus the total number N_s of positive ions produced at the anode will be smaller than those produced when a step pulse is applied. The efficiency will therefore decrease with increase of T_R.

The finite value of efficiency obtained for time delays of 20 μ-sec with a clearing field of 2 kv/cm is easily seen. For clearing fields $<$ 2 kv/cm there is no emission of electrons from the glass whereas all the electrons produced in the gas are removed. The electrons formed in the glass will drift towards the surface and probably remain there until a suitable pulse ($E > 2$ kv/cm) is applied.

Equation (14) shows clearly how the efficiency can vary with the wall thickness of the tube. The reduction in efficiency at low field strengths for the 1.2 mm walled tube (see fig. 21) may be due to the partial shielding of the electric field by the glass dielectric.

Visual evidence showing the existence of filamentary discharge closely resembling streamers is obtained when the tube is photographed transversely during a flash.

In the experiments described in Chapters V and VII the ionising particles were mainly μ-mesons passing through the tubes vertically downwards. The applied field was also in the vertical direction. If the electric field was perpendicular to the direction of the particle there

should be a decrease in the efficiency of the tubes as there can be no emission of electrons from the glass for vertical particles passing along the diameter of the tube. An experiment was therefore made to measure the efficiency of the tubes with the electric field in the horizontal direction while the incident particles were confined to within $\pm 10^{\circ}$ of the zenith. A decrease of $9.0 \pm 1.3\%$ was noticed. The expected 50% decrease was not observed. This may be due to the fact that the horizontal lines of force on entering the spherical surface of the dielectric are refracted at varying angles to the radius of the tube. The direction of the field inside the glass may thus not be horizontal.

However, direct experiments are necessary to show that the initiating electrons leading to later ionisation by collision arise from the disturbed region of the glass. Cloud chamber experiments similar to those performed by Raether (1937) with glass plates covering the electrodes could prove the existence of such emission processes.

In conclusion it appears likely that the streamer mechanism plays at least some part in the functioning of the flash tube. Some further experiments are desirable, but a very detailed examination does not seem profitable since in general the fundamental parameters of the discharge (ionisation coefficient, absorption coefficient, diffusion coefficient, etc.) are not in general accurately known for the experimental conditions used.

CHAPTER IX

THE DESIGN AND CONSTRUCTION OF THE DURHAM SPECTROGRAPH

IX. 1. The Design of the Tube Assemblies

The experiments on the precise location of particle trajectories carried out with the prototype spectrograph described in Chapter VI showed that an overall uncertainty of $(0.62 \pm .10)$ mm could be obtained with five layers of tubes in each array. In order to decrease this value it was decided to use eight layers of tubesin each array. It was necessary that the flash tubes in the four arrays should be arranged in such a manner as to give the minimum positional uncertainty for the location of cosmic rays incident within $\pm$ 10° of the vertical. In order to find this optimum arrangement and the minimum possible value of the positional uncertainty the following procedure was adopted.

Circles to represent the internal sectional area of the tubes were drawn on graph paper. There were eight layers marked 1, 2, 3 ..... as shown in fig. 23. The horizontal separation between the centres of the tubes was 8 mm, the vertical separation being 11 mm. To begin with the tubes were staggered in the simplest manner, the centres of the tubes in the even layers lying midway between the centres of the tubes in the odd layers.

Since it had been found previously that the internal efficiency of the flash tubes was nearly 100% it was assumed that a particle intersecting a tube diameter would fire that tube. With this assumption any ionising particle, represented by the line PQ, incident on the stack at an angle θ to the vertical would fire the tubes shown shaded in fig. 23. The numbers

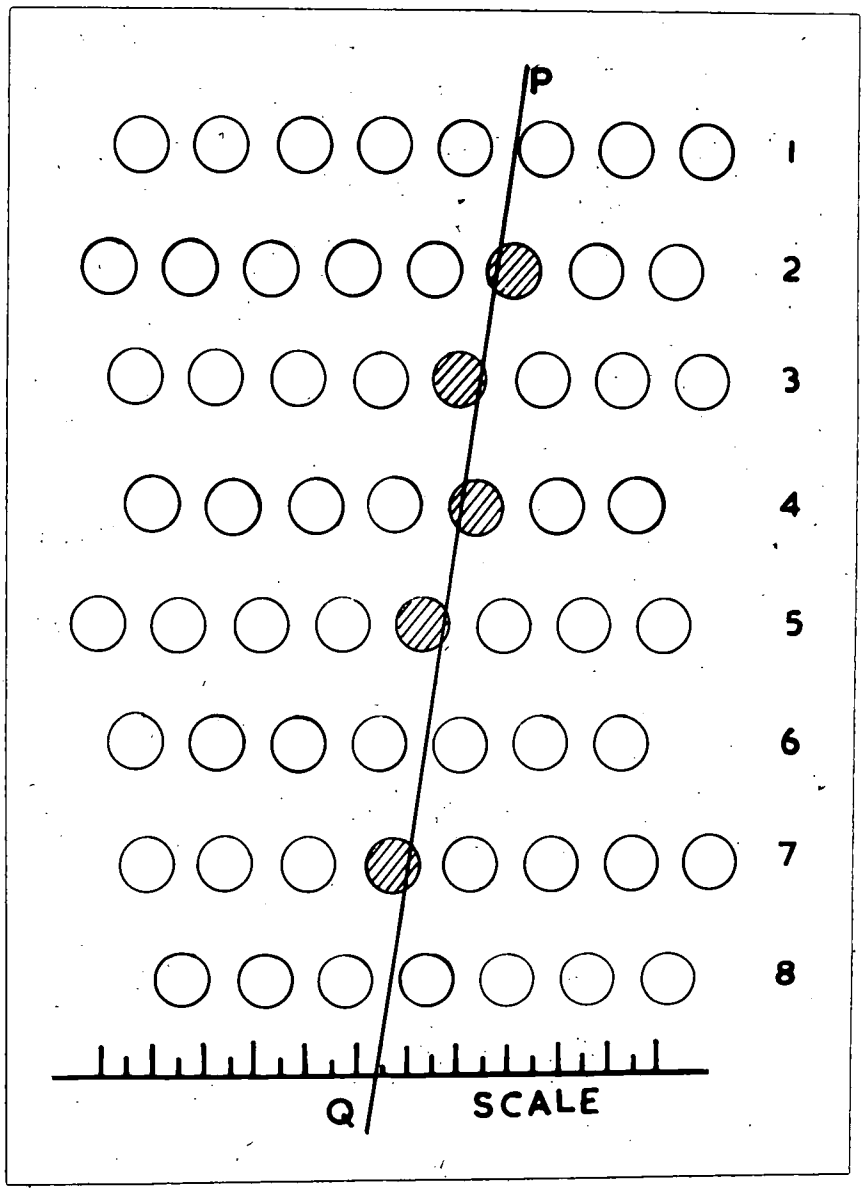

Fig. 23.

A Section Through the Tubes in the Assembly.

of the layers containing these tubes was noted down in a table constructed as shown

TABLE VI

θ°	Tubes discharged	Zero	L.H.	R.H.	Δ in mm	r.m.s. Δ mm.
2	1, 5, 5, 6, 7, 8	100	98.5	101.5	3.0	
2	2, 4, 5, 6, 7, 8	27.5	27.0	28.5	2.25	5.5
-	-	-	-	-	-	

The intersection of the line PQ with the scale at the bottom of the scale in fig. 23 gave the zero reading noted in column 3. The line PQ was then moved parallel to itself until it either missed one of the tubes noted in column 2 or just intersected any new tube. This critical position of the line PQ gave the readings in column 4. The line was then moved to the right until the above criterion was again satisfied. This reading was noted in column 5. The difference between the last two readings gives the value of Δ the overall uncertainty for the ray PQ. Nine readings were taken for each value of θ and the root mean square of Δ calculated. The above procedure was repeated for various values of θ. The r.m.s. value of Δ for the various angles is shown in fig. 24, graph I, curve I. The scale is twice full size. The value of Δ for $\theta = o$ is exactly 4 mm. It is found from the graph that the r.m.s. Δ varies between values of 1.9 mm for $\theta = 4^{\circ}$ and 2.5 mm for $\theta = 10^{\circ}$. The mean value of r.m.s. Δ is found to

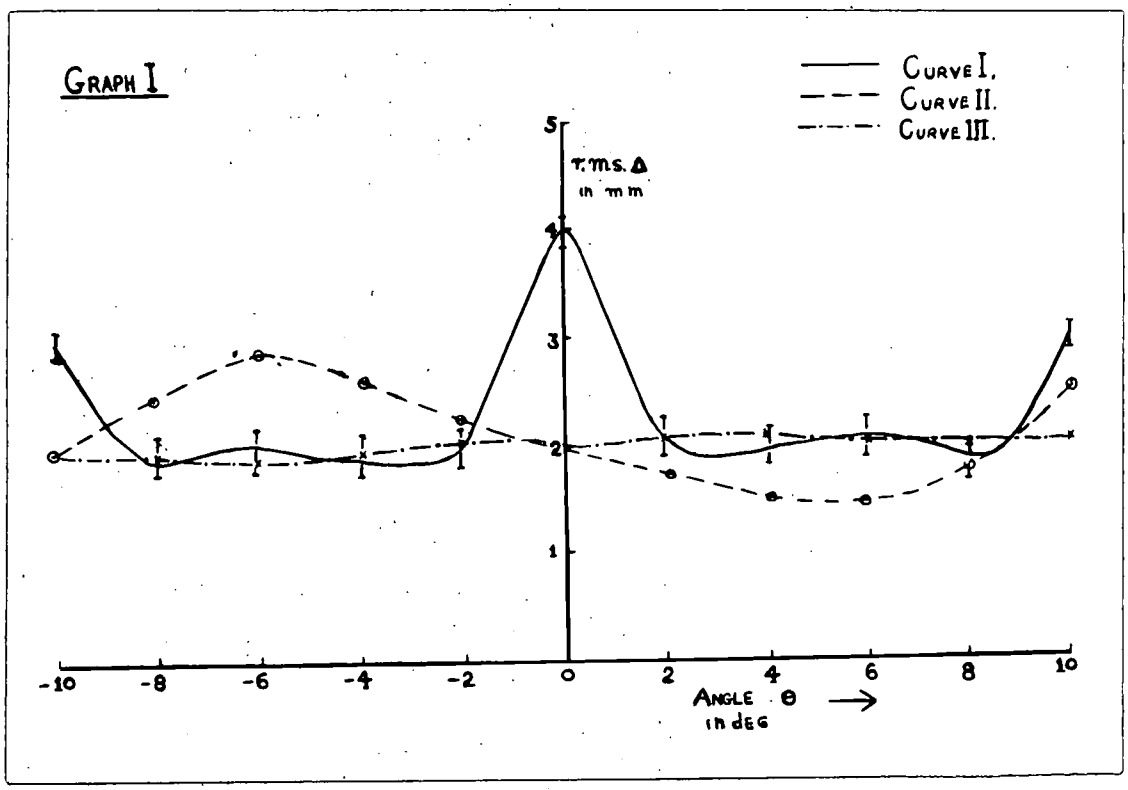

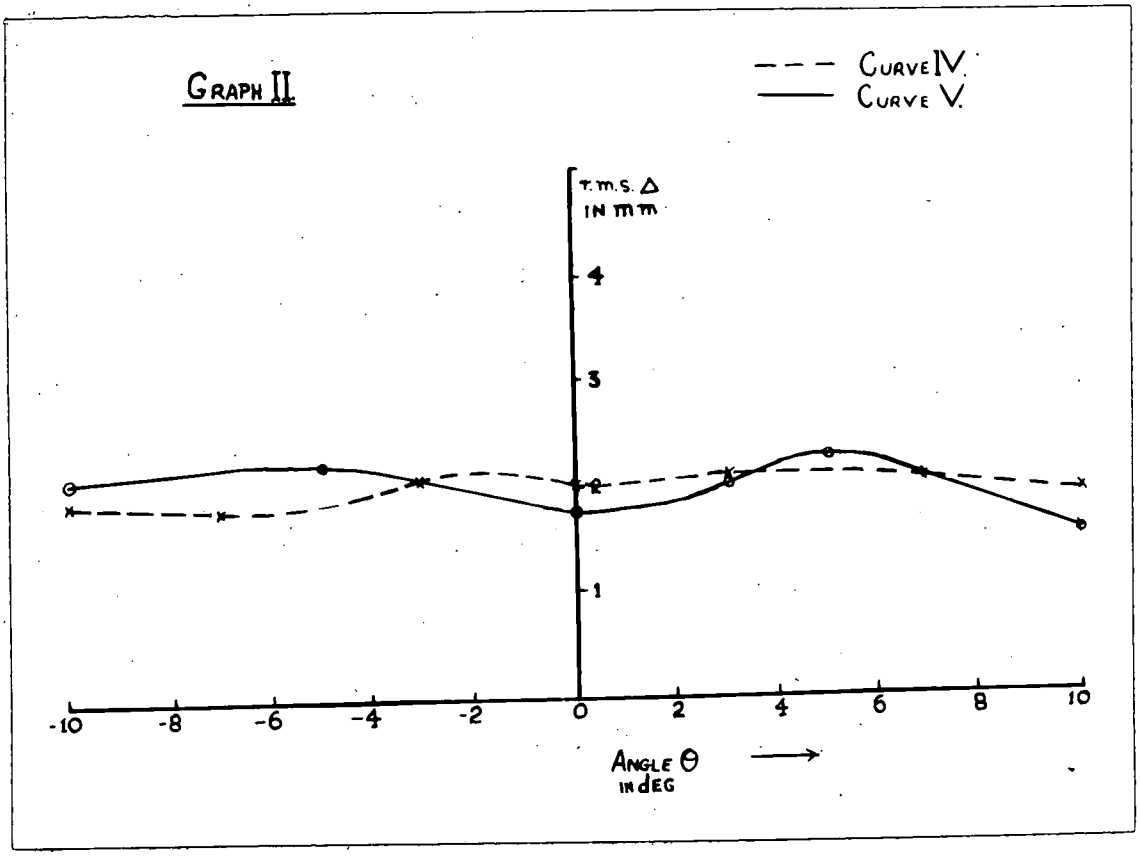

Fig. 24.

The Variation of r.m.s.Δ vs Angle θ (deg)

be 2.2 mm giving a value of 0.31 mm for the standard deviation in the actual arrangement. This is the standard deviation of the mid point of the range of Δ about the true position of the trajectory.

In order to improve on this value and also to give a reasonably flat curve over the range -10° to $+10^{\circ}$, the measurements were repeated with the top four layers displaced to the left by 2 mm. Curve II, Fig. 24 shows the results of these measurements. An asymmetry was found in the curve between the rays incident on one side of the vertical to that on the other. In an attempt to get rid of this asymmetry the measurements were repeated with the four central layers displaced to the left by 2 mm. The results of these measurements are shown in curve III, Fig. 24. The latter curve possesses the desirable feature of being flat over the region $\pm 10^{\circ}$ and also gives a lower value $(0.29 \pm .06)$ mm for the standard deviation.

In theory, a purely random orientation of the tubes should give not only a nearly flat curve but also a lower value of the standard deviation. To test this a subsidiary experiment was performed. Pins were fixed on a portion of a metre rule shown in fig. 25, the space AB representing the internal diameter of the tube and the space BC the dead space which included the walls of two adjacent tubes and the small air gap between them. Eight of these were used to represent the eight layers and were placed one behind the other on a board A. Another board B with pins P, P_1. P_2, fixed as shown in fig. 25 was used to indicate the directions of the incident particles.

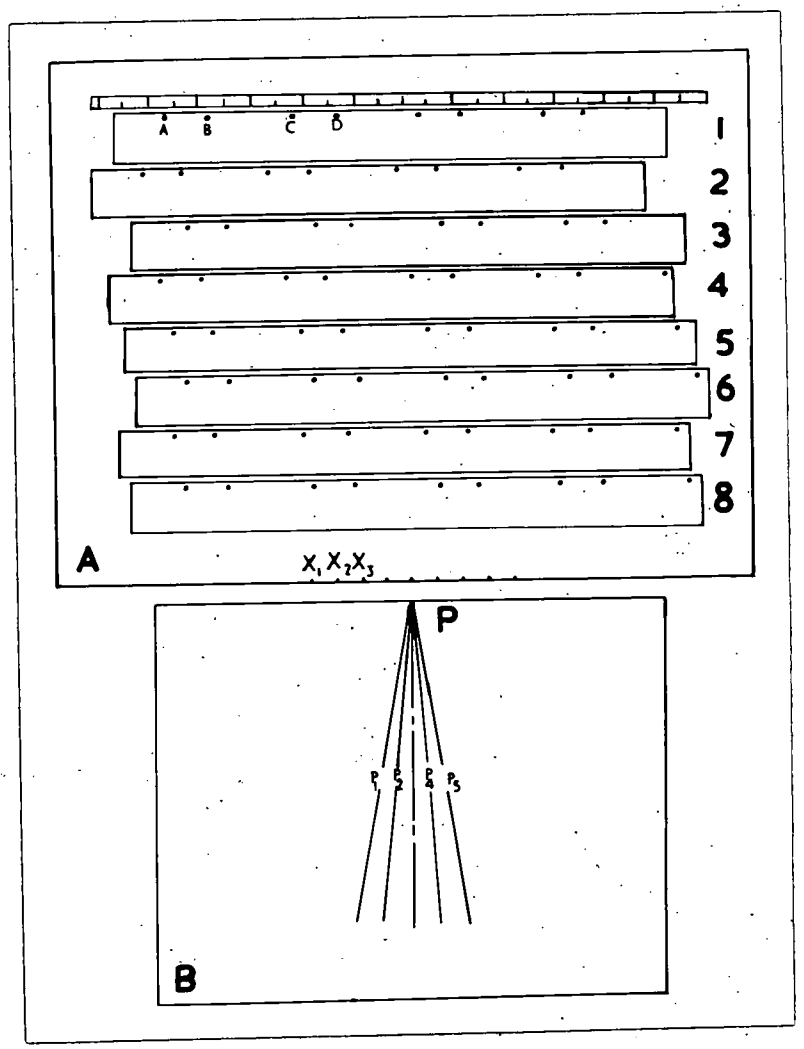

Fig. 25.

The Schematic Diagram of Apparatus used to Test Staggering of Tubes.

To begin with the different layers were adjusted so that on looking in the direction of any of the pins P_1 P, P_2 P, ... etc. the separation of the projections of the pins (on board A) on the scale was a minimum. The position of the nearest pin in each layer from the edge of the board A was noted. The board B was now placed with pin P coincident with the position X, and the separation between the pins when viewed along the directions P_1 P, P_2 P, ... etc. was noted. These give the values of Δ the positional uncertainty for different values of θ. These measurements were repeated for the different positions X_2, X_3... The root mean square value of Δ for each angle θ was plotted to give curve IV, graph II.

This same positioning of the tubes was now reproduced on graph paper and the r.m.s. Δ obtained as described earlier. The results of these measurements are shown in curve V, graph II. Examination of the curves IV and V shows that the values of the standard deviation of the r.m.s. Δ in both cases agree closely. Further, it shows that staggered tubes are as satisfactory or even better than randomly orientated tubes. The former arrangement was therefore incorporated in the actual experimental arrangement.

IX. 2. The Construction and Alignment of Tube Assemblies.

As in the prototype there are four measuring layers A B C and D. The arrangement of these is shown in fig. 26. The tube assembly C is described in detail as the frames A and D are very similar to B and C, their only difference being in size.

A rectangular framework 56 x 33 x 13 cm^3, shown in fig. 27, was first

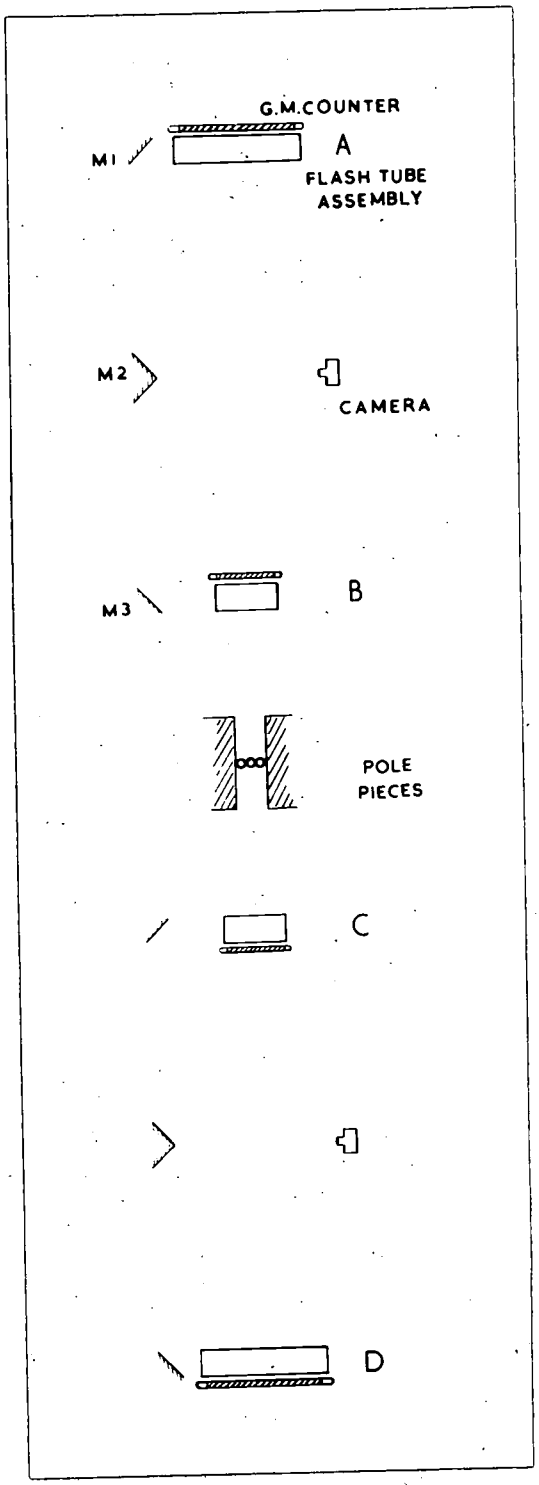

Fig. 26.
The Schematic Diagram of the Durham Spectrograph.

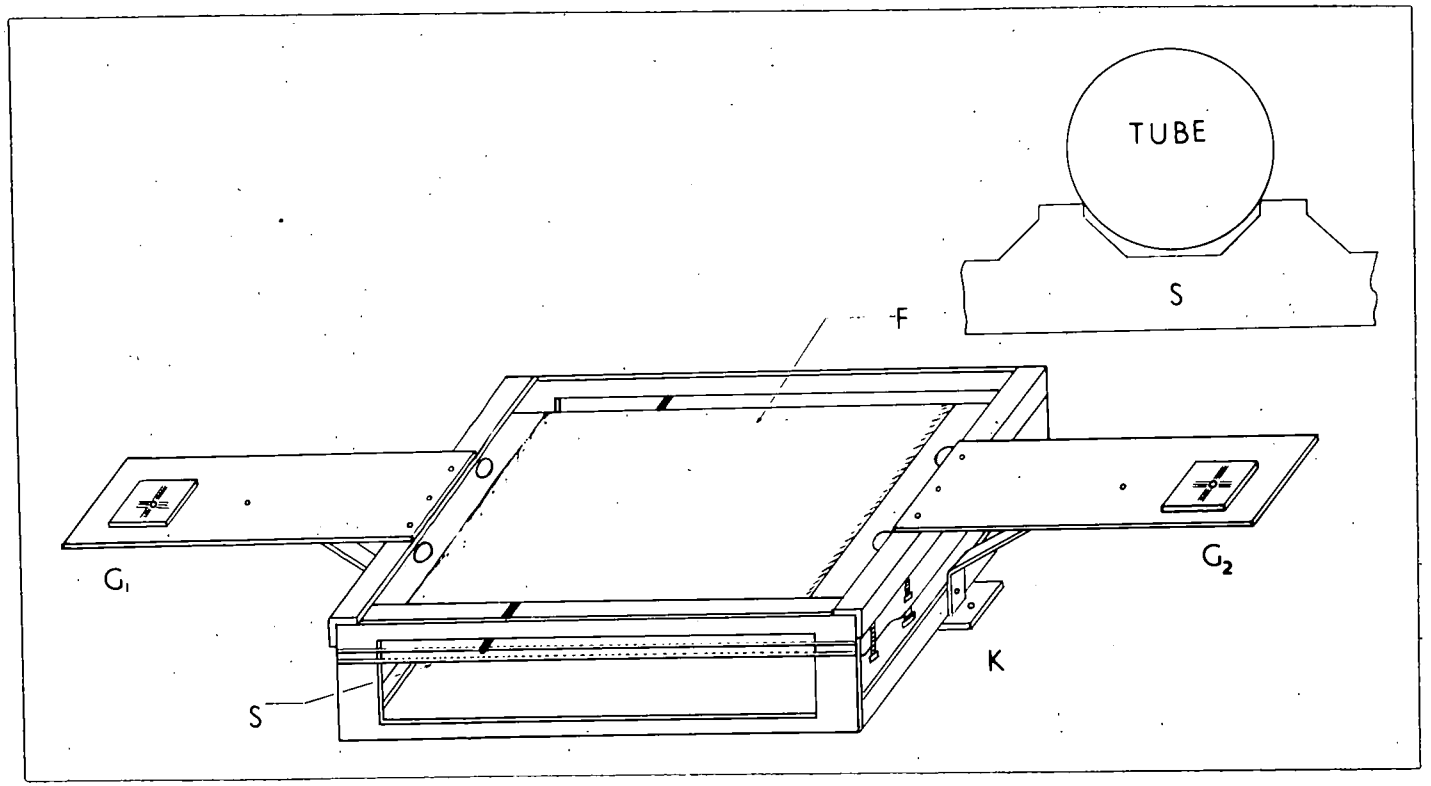

Fig. 27.

An Isometric Projection of Assembly C.

constructed. The slots to carry the tubes are milled in strips of dural and fit into grooves on a $\frac{1}{4}$" plate, the latter being fastened to the front and back plates of the framework. The centres of the slots were separated by (8.0 $\pm$ .01) mm and the vertical separation between the centres of the grooves was (11.5 $\pm$ .01)mm. The profile of the slot was such that selected tubes having external diameter between 7.85 mm and 7.15 mm rested only on two points of the slot. Two layers of tubes were contained within one pair of the electrodes. These were of 10 'thou' aluminium sheets held taut between four brass rods. The high tension plates were well insulated from the framework, the earthed plates being connected directly to the framework. An isometric projection of the tube assembly C and a cross-section of the slot carrying a tube are shown in fig. 27. A photograph of the assemblies A, B and C and the accompanying electronic equipment is shown in fig. 28.

It is essential that the tubes in the various levels be parallel to one another. To achieve this a line perpendicular to the tubes situated symmetrically to the faces of the framework was drawn on the framework. In the region of intersection of this line with the grids G_1 , G_2, two points were chosen. The co-ordinates of these points were known accurately with respect of the grids G_1 and G_2. Holes of 2 mm diameter were drilled with these points as centres. Two plumb lines forming a vertical plane perpendicular to the Geiger counters in the different levels passed through the holes in the four frameworks. By moving the framework until the plumb lines had the same co-ordinates with respect to the grids G_1, G_2 etc. the tubes could be made parallel to one another within $\pm \frac{4}{}$ 'thous'

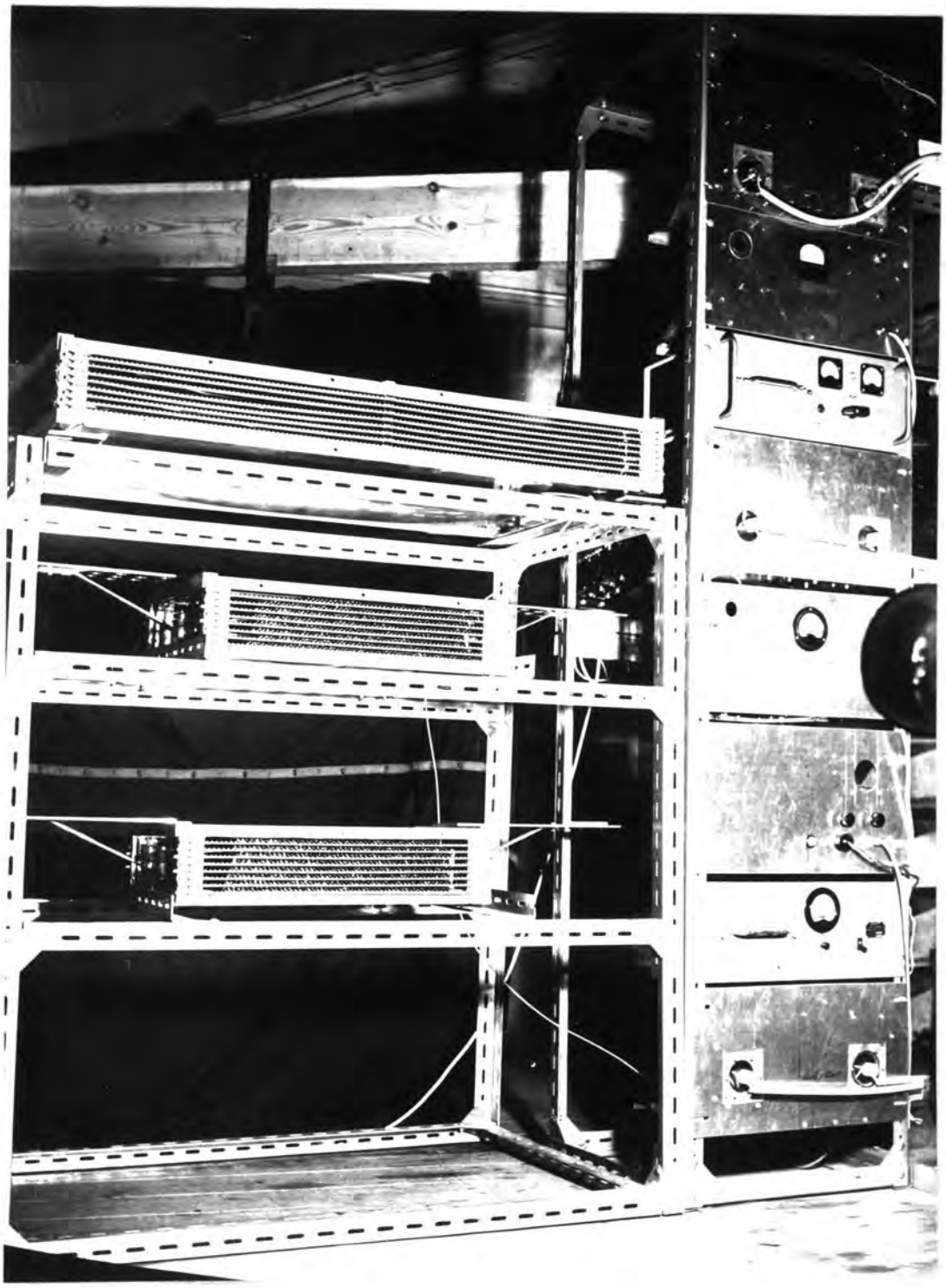

Fig. 28.

Photograph of the Assemblies A, B, C and the Electronic Equipment

The frames containing the tubes in the four levels were kinematically located in the conventional manner.

A mirror system (Fig. 26) M_1 , M_2, M_3 enables the flashes of the tubes in the levels A and B to be photographed on the same film.

IX. 3. General Remarks and Future Work

Using the value of the standard deviation for the overall uncertainty obtained in Chapter IX. 1, the maximum detectable momentum of the spectrograph is estimated to be $\sim$800 G.e.v/$_c$. The displacement of any fast particle due to scattering in the instrument is $\sim$4% of the displacement due to the deflection in the magnetic field.

In conclusion it may be said that the prototype spectrograph described in Chapter VI has been operated successfully in Nottingham, and measurements of the momentum spectrum of 1,000 particles have been made. The Durham Spectrograph is nearly ready and it is expected that measurements on the spectrum and the positive - negative ratio of fast particles will soon be made.

ACKNOWLEDGEMENTS

The author is greatly indebted to Professor G. D. Rochester, F.R.S. for his support and constant interest in the work.

He is very grateful to Dr. A. W. Wolfendale for the guidance, help and constant interest in the work.

The author wishes to thank his colleagues, Messrs. M. Gardener, F. Ashton, D. G. Jones, H. Coxell and J. L. Lloyd for their helpful co-operation.

The author wishes to thank the members of the workshop staff, Messrs. M. Cutter, D. Jobling, M. Crossland, L. Edwards. R. Stark and H. Fettis for their assistance in the construction of the spectrograph.

The Department of Scientific and Industrial Research is thanked for their award of a student research assistantship for the period 1956-1958.

APPENDIX I

Statistical Treatment of the Flash Tube Data.

The problem is to derive the best estimate of flash tube efficiency and its standard deviation. Consider the case where we have a layer of tubes and single cosmic rays passing through. If in an experiment there are 'a' flashes and 'b' blanks then we define the layer efficiency, η, as

$$\eta = \frac{a}{a+b}$$

Now a and b are both distributed according to Poisson statistics so that the standard deviationof a is $\sqrt{a}$ and b is $\sqrt{b}$. Thus we have

$$\frac{1}{\eta} = 1 + \frac{b}{a}$$

$$-\frac{d\eta}{\eta^2} = \frac{a\,db - b\,da}{a^2}$$

$$= \frac{b}{a}\left\{\frac{db}{b} - \frac{da}{a}\right\}$$

i.e. substituting for $\frac{b}{a}$ we have

$$-\frac{d\eta}{\eta^2} = \left(\frac{1}{\eta} - 1\right)\left\{\frac{db}{b} - \frac{da}{a}\right\}$$

$$-\frac{d\eta}{\eta^2} = \left(\frac{1-\eta}{\eta}\right)\left(\frac{db}{b} - \frac{da}{a}\right)$$

$d\eta$, db, da are small differentials in calculus notation and we square and add independently to find the standard deviation

i.e.

$$\frac{\langle d\eta^2 \rangle}{\eta^2} = (1-\eta)^2 \left\{ \frac{\langle db^2 \rangle}{b^2} + \frac{\langle da^2 \rangle}{a^2} \right\}$$

But

$$\frac{\langle db^2 \rangle}{b^2} = \frac{1}{b} \quad \text{and} \quad \frac{\langle da^2 \rangle}{a^2} = \frac{1}{a}$$

Since the standard deviation of a is $\sqrt{a}$ we have

$$\frac{d\eta}{\eta} = (1-\eta)\frac{1}{\sqrt{\eta b}} = \frac{\sqrt{1-\eta}}{\sqrt{a}}$$

Changing the notation to n flashes out of N frames we have

$$d\eta = \frac{\eta\sqrt{1-\eta}}{\sqrt{n}} = \frac{\sqrt{\eta(1-\eta)}}{\sqrt{N}}$$

Thus the efficiency is given by

$$\eta = \frac{n}{N} \pm \frac{\sqrt{\eta(1-\eta)}}{\sqrt{N}}$$

REFERENCES

Alikanian A., Alikana A., and Weissenberg A.	1947.	J. Phys U.S.S.R. 11. 97.
Ashton F., Kisdnasamy S. and Wolfendale A. W.	1958.	Nuovo Cimento 8. 615
Barsanti G., Conversi M., Focardi S., Murtas G. P. Rubia C., and Torelli G.	1956	Proceedings of C.E.R.N. symposium 11. 56.
Blondi M. A., and Brown S. C.	1949	Phy. Rev 76 1697
Blackett P. M. S.	1937	Proc. Roy. Soc. A 159 1
Caro D. E., Parry J. K., and Rathegeber H.	1951	Aust. J. Sc. Res. A 4 16.
Conversi M. & Gozzini A.	1955	Nuovo Cimento 2 189
Cranshaw T. E. & de Beer J. F.	1957	Nuovo Cimento 5 1107
Druvestyn M. J. & Penning F M.	1940	Rev. Mod. Phy. 12 87.
Ehmert A.,	1957	Zeitz. f. Physik 106 751
Eyeions D. A., Owen B. G., Price B T. and Wilson J. G.	1955	Proc. Phy. Soc. A. 68 795
Gardener M., Kisdnasamy S., and Wolfendale A. W.	1957	Porc. Phy. Soc. B. LXX. 687
Healey R. H. & Reed R. W.	1941	The behaviour of slow electrons in gases (Sydney Amalgamated Wireless of Australia.
Hess. R.,	1912	Phys. Zeits 13 1084.

Holmes J. E. R., Owen B. G., Rodgers A. L., Wilson J. G.	1955	Report of the conference on recent developments in cloud chamber and associated techniques (London: University College)
Hyams B. O., Mylroi M. G. Owen B. G. & Wilson J. G.	1950	Proc. Phy. Soc. A63 1053
Jesse W. P. & Sadauskis J.	1952	Phy. Rev. 88 417
Jones H.	1939	Rev. Mod. Phy. 11 235.
Kolhorster D.	1914	Phys. Ges., Verhandlungen 719.
Lloyd J. L., Rossle E., & Wolfendale A. W.	1957	Proc. Phys. Soc. A 70 421
Lloyd J. L.	1958	(To be published).
Loeb L. B.	1939	Fundamental Processes in electrical discharge in gases (John Wiley and Sons).
Loeb L. B. and Meek J. M.	1941	The mecahnism of the electric spark (Stanford University Press)
Loeb L. B.	1948	Proc. Phy. Soc. 60 561
Meek J. M.	1940	Phy. Rev. 57 722
Meek J. M. and Craggs J D.	1955	Electrical breakdown of gases (Oxford, at the Clarendon Press).
Pidd R. W. & Madansky L.	1949	Phy. Rev. 75 1175
Raether H.	1937	Z. Physik 107 91.
Raether H.	1940	Arch. Electrotech 20 49.

Rittner E.S.	1948	Phy. Rev. 73 1212
Robinson E.	1953	Proc. Phy. Soc. A 66 73
Rossi B. & Staub H. H.	1949	Ionisation chambers and counters (New York McGraw Hill).
Slepian J., and Berkey W. E.	1940	J. Appl. Phys 11 765
Wilson J. G.	1955	Proc. Phy. Soc. A 68 795
Wilson V C	1938	
Wilson J. G	1946	